

REVIEW ARTICLE

On growth, disorder, and field theory

Michael Lässig

Max-Planck-Institut für Kolloid- und Grenzflächenforschung Kantstrasse 55, 14513 Teltow, Germany†

Received 7 August 1998

Abstract. This article reviews recent developments in statistical field theory far from equilibrium. It focuses on the Kardar–Parisi–Zhang equation of stochastic surface growth and its mathematical relatives, namely the stochastic Burgers equation in fluid mechanics and directed polymers in a medium with quenched disorder. At strong stochastic driving—or at strong disorder, respectively—these systems develop *non-perturbative* scale invariance. Presumably exact values of the scaling exponents follow from a self-consistent asymptotic theory. This theory is based on the concept of an *operator product expansion* formed by the local scaling fields. The key difference from standard Lagrangian field theory is the appearance of a *dangerous irrelevant* coupling constant generating *dynamical anomalies* in the continuum limit.

Contents

- 1 Introduction
 - 1.1 Directed growth, the Burgers equation, and polymers
 - 1.2 Overview of this article
- 2 The field theory of directed strings
 - 2.1 Correlation functions and the operator product expansion
 - 2.2 Renormalization
 - 2.3 Results and discussion
- 3 Directed strings in a random medium
 - 3.1 Replica perturbation theory
 - 3.2 The strong-coupling regime
 - 3.3 A string and a linear defect
 - 3.4 A string and a wall
 - 3.5 Strings with mutual interactions
 - 3.6 The upper critical dimension of a single string
 - 3.7 Discussion
- 4 Directed growth
 - 4.1 Field theory of the Kardar–Parisi–Zhang model
 - 4.2 Dynamical perturbation theory
 - 4.3 Renormalization beyond perturbation theory
 - 4.4 Response functions in the strong-coupling regime
 - 4.5 Height correlations in the strong-coupling regime
 - 4.6 The dynamical anomaly and quantized scaling
 - 4.7 Discussion

† E-mail: lassig@mpikg-teltow.mpg.de.

1. Introduction

The last 25 years have seen a very fruitful application of continuum field theory to statistical physics [1]. A system in thermodynamic equilibrium tuned to a critical point ‘looks the same on all scales’; that is, it shows an enhanced symmetry called scale invariance. Since there is no characteristic scale, the correlation functions in a critical system can only be power laws. Microscopically quite different systems share certain aspects of their critical behaviour which are therefore independent of the small-scale details. This phenomenon is called universality. Among the universal features are the exponents characterizing the power laws of correlation functions.

The renormalization group has provided the first satisfactory explanation of universality as well as calculational tools to compute, for example, critical exponents. The central concept is that of a flow on the ‘space of theories’. In equilibrium systems, this flow is parametrized by the coupling constants of an effective Hamiltonian determining the partition function. It can be understood as a link between the microscopic coupling constants defining a model and the effective parameters governing its large-distance limit. (For an Ising model, e.g., the former are the spin couplings on the lattice and the latter are the reduced temperature and the magnetic field.) The fixed points of this flow represent the universality classes. At a fixed point, a system can be described by a so-called renormalized continuum field theory, that is, a theory where all microscopic quantities such as the underlying lattice constant no longer play any role. The universal properties can often be calculated in a systematic perturbation expansion.

About a decade after Wilson’s seminal work on renormalization, the advent of conformal field theory triggered a new interest in two-dimensional critical phenomena [2]. It was realized that these systems have an even larger symmetry called conformal invariance. (A conformal transformation is any coordinate transformation that *locally* reduces to a combination of scale transformation, rotation and translation. The rescaling factor is now allowed to vary from place to place.) Conformal invariance severely constrains the structure of continuum field theories in two dimensions, yielding a (partial) classification of the universality classes and their exact scaling properties. Under some additional conditions, there is only a discrete set of solutions: the possible values of the critical exponents are *quantized*.

The subsequently developed S -matrix theory has extended the exact solvability to theories close to a critical point, i.e., with a large but finite correlation length. For the first time, it has been possible to verify the ideas of scaling beyond perturbation theory for a whole class of strongly interacting field theories. On the other hand, the conformal formalism entails a shift of focus from *global* quantities (such as the Hamiltonian of a theory and its coupling constants) to *local* observables, i.e., the correlation functions. Their structure is encoded by the so-called operator product expansion, a rather formidable name for a simple concept (explained in section 2). The operator product expansion is at the heart of a field theory. Conformal symmetry imposes a set of constraints on the operator product expansion which lead to expressions for the correlation functions. This theory makes no reference to a Hamiltonian. Without a renormalization group flow, however, the link to microscopic model parameters is lost. Hence, it has to be determined *a posteriori* which lattice models belong to the universality class of a given conformal field theory.

Another important shift of focus has taken place in recent years. Traditionally, scale invariance has been associated with second-order phase transitions, which requires fine-tuning of the model parameters to a critical manifold. However, it became clear that

there are many systems that have generic scale invariance in a region of their parameter space. Perhaps the simplest such systems are interfaces. For example, the surface of a crystal in thermal equilibrium fluctuates around an ideal symmetry plane of the crystal. The displacement can be described by the ‘height’ field $h(\mathbf{r})$, the two-dimensional vector \mathbf{r} denoting the position in the reference plane. Above a certain temperature, the surface is rough, i.e., it develops mountains and valleys whose size is typically some power of the system size. The correlation functions of the height field become power laws as well. The roughness turns out to be even stronger if the crystal is growing, which drives the surface out of equilibrium. There is another important difference between equilibrium surfaces and driven surfaces. In the former case, the height pattern shows an up–down symmetry between mountains and valleys. Out of equilibrium, that symmetry is lost.

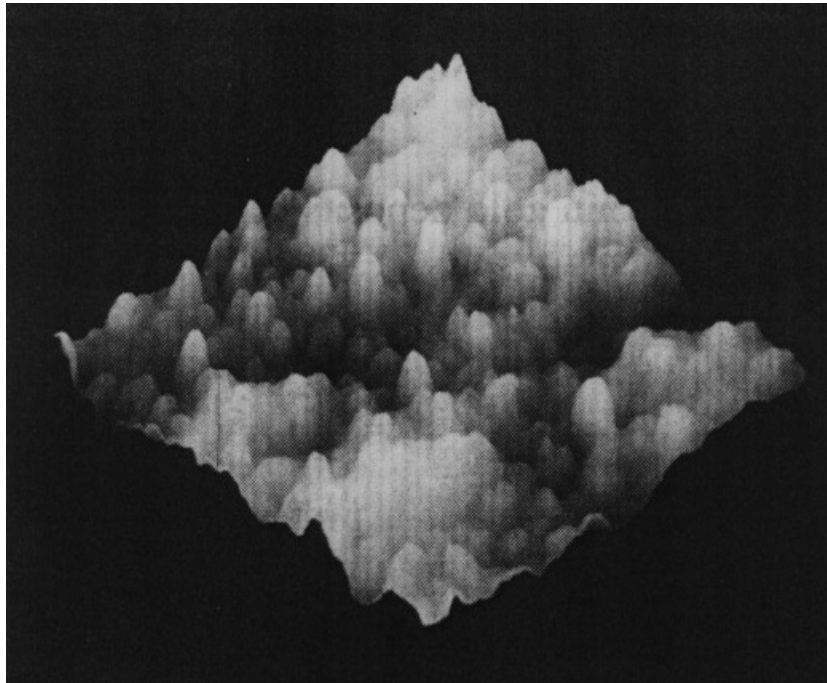
Obviously, such open systems are quite common: any growth, pattern formation or reaction process propagating through some localized boundary or front generates a driven interface, often with long-ranged correlations [3, 4]. An example is the kinetic roughening of thin metal films by vapour deposition. Figure 1(a) shows the ST microscope analysis of a gold film at room temperature from which the authors were able to extract power-law behaviour of the height correlations, indicative of a scale-invariant surface state [5].

This state is seen to be *directed* (i.e., it has no up–down symmetry) and *stochastic*. Surface inhomogeneities increase with time, signalling a *non-linear* evolution. However, since there are no significant overhangs, the growth mechanism should be essentially *local*; that is, the growth rate at a given point depends only on the surface pattern in the neighbourhood of that point. (Kinetic roughening can also produce quite different surface patterns with branched tree-like structures. Their growth is strongly non-local since the large trees shield the smaller ones from further deposition of material [6].)

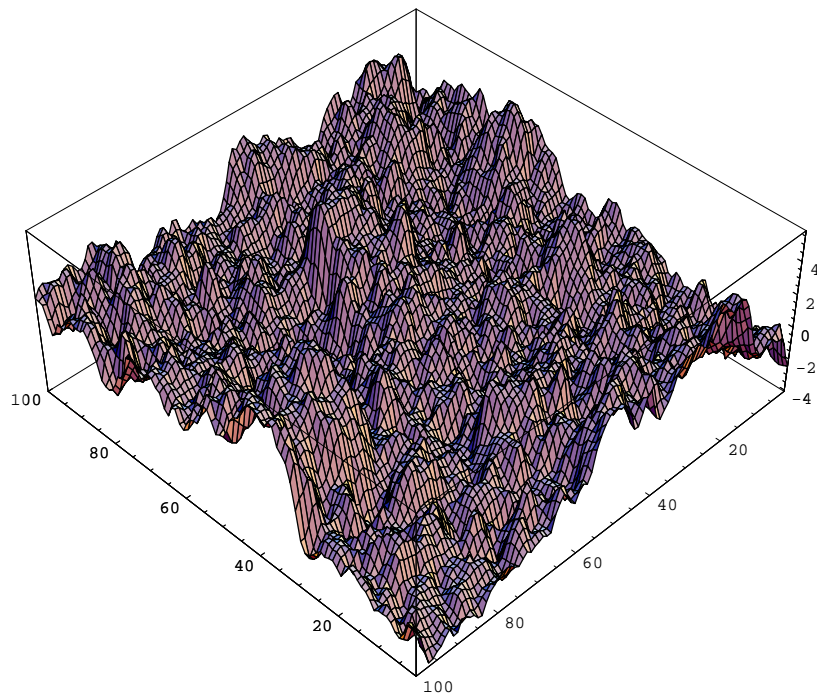
Of course, generic scale invariance far from equilibrium is not limited to interfaces. Other important examples are hydrodynamic turbulence or slowly driven systems with so-called self-organized criticality: dynamical processes such as the stick–slip motion of an earthquake fault generate a power-law distribution of ‘avalanches’ with long-ranged correlations in space and time. A simple lattice model with a self-organized critical state is the so-called forrest fire model [7, 8]. On a given lattice site, a tree grows with a small probability per unit time. With an even smaller probability, the tree is hit by a lightning strike which destroys it along with all of the trees in the same contiguous forrest cluster [8]. These events are the avalanches. The dynamics leads to a self-similar stationary pattern of forrests and voids.

A satisfactory theory of non-equilibrium scale invariance should classify the different universality classes and provide calculational methods for obtaining the scaling exponents exactly or in a controlled approximation. To establish such a theory is obviously a complex task that will challenge statistical physicists probably over the next 25 years. The power-law correlations on large scales of space and time should again be described by continuum field theories, although the proper continuum formulation is far from clear for many dynamical systems defined originally on a lattice. It is also an open issue which of the currently known field-theoretic concepts will continue to play an important role. For example, perturbative renormalization may fail to produce a fixed point describing the large-distance regime, as will be shown below for the example of driven surface growth. The seemingly easier task of describing the time-independent scaling in a stationary state is still involved since there is no simple Hamiltonian generating these correlations.

This article collects a few results that may become part of an eventual field theory of non-equilibrium systems. We limit ourselves to models related to the Kardar–Parisi–Zhang



(a)



(b)

Figure 1. (a) A STM snapshot of a kinetically roughened gold film. The projected area of the sample is $510 \times 510 \text{ nm}^2$. Courtesy of Herrasti *et al* [5]. (b) Part of a discretized KPZ surface. The entire surface has 400×400 lattice points and is shown after 1000 time steps.

(KPZ) equation [9]

$$\partial_t h(\mathbf{r}, t) = v \nabla^2 h(\mathbf{r}, t) + \frac{\lambda}{2} (\nabla h(\mathbf{r}, t))^2 + \eta(\mathbf{r}, t) \quad (1.1)$$

for a d -dimensional height field $h(\mathbf{r}, t)$ driven by a force $\eta(\mathbf{r}, t)$ random in space and time. This equation has come to prominence as the ‘Ising model’ of non-equilibrium physics. It is indeed the simplest equation capturing nevertheless the main determinants of the growth dynamics in figure 1(a): *directedness, non-linearity, stochasticity, and locality*. The KPZ surface shown in figure 1(b) has been produced by a discretized version of the growth rule (1.1) and looks indeed qualitatively similar to these experimental data.

The theoretical richness of the KPZ model is partly due to close relationships with other areas of statistical physics—notably hydrodynamic turbulence and disordered systems—which are briefly reviewed below. Many more details can be found in references [3, 4]. Due to the famous problem of quenched averages, disordered systems share some of the conceptual problems mentioned above. The observables are correlation functions averaged over the distribution of the random variables, which is not given by a Boltzmann weight. These correlations may be regarded as an abstract field theory but there is again no simple effective Hamiltonian. Such systems can have scale-invariant states at zero temperature for which the very existence of a continuum limit needs to be re-established.

Despite considerable efforts, the KPZ equation has so far defied attempts at an exact solution or a systematic approximation for dimension $d > 1$. The main reason for this is the failure of renormalized perturbation theory. Renormalization aspects of equation (1.1) and its theoretical relatives will be discussed below. The main emphasis lies, however, on structures beyond perturbation theory. We analyse the internal consistency of the strong-coupling field theory expressed by the operator product expansion of its local fields. This approach turns out to be quite powerful. Using phenomenological constraints and the symmetries of the equation, it produces a quantization condition on the scaling indices from which their exact values for $d = 2$ and $d = 3$ can be deduced. This quantization is somewhat reminiscent of what happens in conformal field theory and suggests that the KPZ equation possesses an infinite-dimensional symmetry as well.

It is not clear to what extent the results carry over to other non-equilibrium systems. Yet, the approach used here is fairly general and should be applicable in a wider context. It transpires that incorporating non-equilibrium phenomena into the framework of field theory will require yet another shift of focus to non-perturbative concepts and methods. This is likely to change our view of field theory as well. Negative scaling dimensions, dangerous variables, anomalies etc are oddities today but may become an essential part of its future shape.

1.1. Directed growth, the Burgers equation, and polymers

The time evolution of a KPZ surface depends only on the local configuration of the surface itself (and not, for example, on the bulk system beneath the surface). Hence, the r.h.s. of equation (1.1) contains only terms that are invariant under translations $h \rightarrow h + \text{constant}$.

(a) The dissipation term $\nabla^2 h$ is the divergence of a downhill current and acts to smooth out the inhomogeneities of the height field.

(b) The non-linear term $(\nabla h)^2$ arises from expanding the tilt dependence of the local growth rate and acts to increase the inhomogeneities of the surface. A linear term $\mathbf{b} \cdot \nabla h$ would be redundant since it could be absorbed into a tilt $h \rightarrow h + \mathbf{b} \cdot \mathbf{r}$. The higher powers

$(\nabla h)^3, \dots$ turn out to be irrelevant in the presence of the quadratic term, as well as terms containing higher gradients such as $(\nabla^2 h)^2$ or $\nabla^4 h$.

(c) The stochastic driving term $\eta(\mathbf{r}, t)$ describes the random adsorption of molecules onto the surface. It is taken to have a spatially uniform Gauss distribution with correlations only over microscopic distances:

$$\overline{\eta(\mathbf{r}, t)} = 0 \quad \overline{\eta(\mathbf{r}, t)\eta(\mathbf{r}', t')} = \sigma^2 \delta(\mathbf{r} - \mathbf{r}')\delta(t - t'). \quad (1.2)$$

A uniform average $\overline{\eta(\mathbf{r}, t)} = \bar{\eta}$ would again be redundant since it could be absorbed into the transformation $h(\mathbf{r}, t) \rightarrow h(\mathbf{r}, t) - \bar{\eta}t$.

Equation (1.1) is by no means the only model for a driven surface, and many experimental realizations of crystal growth are probably governed by related equations with additional symmetries and conservation laws [10] or with different correlations of the driving force (see, for example, [11]). As the simplest non-linear model, however, the KPZ equation remains a cornerstone for the theoretical understanding of stochastic growth.

The morphology of a rough surface is characterized by the asymptotic scaling of the spatio-temporal height correlations. In a stationary state, the mean square height difference is expected to take the form

$$\langle (h(\mathbf{r}_1, t_1) - h(\mathbf{r}_2, t_2))^2 \rangle \sim |\mathbf{r}_1 - \mathbf{r}_2|^{2\chi} \mathcal{G}\left(\frac{t_1 - t_2}{|\mathbf{r}_1 - \mathbf{r}_2|^z}\right). \quad (1.3)$$

The higher moments $\langle (h(\mathbf{r}_1, t_1) - h(\mathbf{r}_2, t_2))^k \rangle$ are of similar form. (In a system of finite size R , equation (1.3) is valid for $|\mathbf{r}_1 - \mathbf{r}_2| \ll R$ and $|t_1 - t_2| \ll R^z$.) The scaling function \mathcal{G} parametrizes the crossover between the power laws $\langle (h(\mathbf{r}_1, t) - h(\mathbf{r}_2, t))^2 \rangle \sim |\mathbf{r}_1 - \mathbf{r}_2|^{2\chi}$ and $\langle (h(\mathbf{r}, t_1) - h(\mathbf{r}, t_2))^2 \rangle \sim |t_1 - t_2|^{2\chi/z}$ of purely spatial and purely temporal correlations, respectively. These relations define the roughness exponent $\chi > 0$ and the dynamic exponent z . In the marginal case ($\chi = 0$), the surface may still be logarithmically rough.

A surface governed by the linear dynamics (1.1) with $\lambda = 0$ has $\chi = (2 - d)/2$ and $z = 2$: it is rough for $d = 1$, marginally rough for $d = 2$, and smooth for $d > 2$. The phase diagram is well known also for $\lambda \neq 0$. For dimension $d \leq 2$, any small non-linearity $(\lambda/2)(\nabla h)^2$ is a relevant perturbation of the linear theory and induces a crossover to a different rough state called the strong-coupling regime. For $d > 2$, a small non-linearity does not alter the smooth state of a linear surface. There is now a roughening transition to the strong-coupling regime at finite values $\pm\lambda_c$ [12–14].

This phase diagram corresponds to the following renormalization group flow. For $d \leq 2$, the Gaussian fixed point ($\lambda = 0$) is (infrared-) unstable, and there is a crossover to the stable strong-coupling fixed point. For $d > 2$, a third fixed point exists, which represents the roughening transition. It is unstable and appears between the Gaussian fixed point, and the strong-coupling fixed point which are now both stable [15–18].

In one dimension, the critical indices of the strong-coupling regime take the exact values $\chi = 1/2$ and $z = 3/2$ [19, 9, 20]. Their values for higher dimensions as well as the properties of the roughening transition have been known only numerically [21–28] and in various approximation schemes [29–31]. In particular, it has been controversial whether there is a finite upper critical dimension $d_>$ at and above which KPZ surfaces are only marginally rough ($\chi = 0$ and $z = 2$). These issues are discussed in detail in sections 3 and 4.

Experiments on growing surfaces require delicacy since crossover and saturation effects can mask the asymptotic scaling. However, several experiments have produced scaling consistent with KPZ growth. The fire fronts in slow combustion of paper have $\chi = 0.50$ and $z = 1.53$ [32], in very good agreement with the KPZ values for $d = 1$. A recent study

of kinetically roughened Fe/Au multilayers [33] obtains $\chi = 0.43 \pm 0.05$, which should be compared to the current numerical estimate $\chi \approx 0.39$ for $d = 2$ and to the presumably exact value (4.74).

Equation (1.1) is formally equivalent to Burgers' equation

$$\partial_t \mathbf{v} + (\mathbf{v} \cdot \nabla) \mathbf{v} = \nu \nabla^2 \mathbf{v} + \nabla \eta \tag{1.4}$$

for the driven dynamics of the vortex-free velocity field $\mathbf{v}(\mathbf{r}, t) = \nabla h(\mathbf{r}, t)$ describing a randomly stirred fluid (with $\lambda = -1$) [19]. In this formulation, Galilei invariance becomes obvious: the substitutions

$$h(\mathbf{r}, t) \rightarrow h(\mathbf{r} - \mathbf{u}t, t) + \mathbf{u} \cdot \mathbf{r} - \frac{1}{2} \mathbf{u}^2 t \quad \mathbf{v}(\mathbf{r}, t) \rightarrow \mathbf{v}(\mathbf{r} - \mathbf{u}t, t) + \mathbf{u} \tag{1.5}$$

leave equations (1.1) and (1.4) invariant. Due to this invariance, the roughness exponent and the dynamical exponent obey the scaling relation [34]

$$\chi + z = 2 \tag{1.6}$$

which guarantees that the total derivative $d_t \equiv \partial_t + \mathbf{u} \cdot \nabla$ behaves consistently under scale transformations.

It should be emphasized, however, that the velocity field of a stirred Burgers fluid looks quite different from the gradient field of a KPZ surface since the driving force in a fluid is correlated over *macroscopic* spatial distances R . This generates turbulence [35] (somewhat different, of course, from Navier–Stokes turbulence). The velocity correlations show multiscaling. For example, the stationary moments $\langle (v_{\parallel}(\mathbf{r}_1) - v_{\parallel}(\mathbf{r}_2))^k \rangle$ of the longitudinal velocity difference have a k -dependent singular dependence on R for $|\mathbf{r}_1 - \mathbf{r}_2| \ll R$. Multiscaling is not expected for driving forces with short-ranged correlations (1.2). This point will become important below.

Via the well-known Hopf–Cole transformation

$$Z(\mathbf{r}, t) \equiv \exp \left[\frac{\lambda}{2\nu} h(\mathbf{r}, t) \right] \tag{1.7}$$

equation (1.1) can be mapped onto the imaginary-time Schrödinger equation

$$\beta^{-1} \partial_t Z = \frac{\beta^{-2}}{2} \nabla^2 Z + \lambda \eta Z \tag{1.8}$$

with $\beta = 1/2\nu$ [9]. The solution can be represented as a path integral

$$Z(\mathbf{r}', t') = \int \mathcal{D}\mathbf{r} \delta(\mathbf{r}(t') - \mathbf{r}') \exp(-\beta S) \tag{1.9}$$

with the action

$$S = \int^{t'} dt \left(\frac{1}{2} \left(\frac{d\mathbf{r}}{dt} \right)^2 - \lambda \eta(\mathbf{r}(t), t) \right) \tag{1.10}$$

describing a *string* or directed polymer $\mathbf{r}(t)$ (i.e., the world line of a random walk) in the quenched random potential $\lambda \eta(\mathbf{r}, t)$ at temperature $\beta^{-1} = 2\nu$. A configuration of the string is shown in figure 2. The stochastic driving term now appears as quenched disorder in a $(1 + d)$ -dimensional equilibrium system. This system is of conceptual importance as one of the simplest problems with quenched disorder.

The transverse displacement of the string

$$\overline{\langle (\mathbf{r}(t_1) - \mathbf{r}(t_2))^2 \rangle} \sim |t_1 - t_2|^{2\zeta} \tag{1.11}$$

defines its roughness exponent ζ . (Averages over the disorder are denoted by overbars, thermal averages by brackets, $\langle \dots \rangle$.) The rough strong-coupling regime (1.3) of the growing

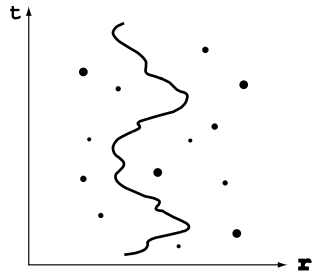


Figure 2. A configuration $r(t)$ of a string (or directed polymer) in a medium with quenched point disorder. Due to the inhomogeneities of the medium, a typical path takes larger excursions to the left and to the right than an ordinary random walk.

surface corresponds to a superdiffusive state of the string ($\zeta > 1/2$) [36–38]. In this state, the universal part of its free energy in a system of longitudinal size L and transverse size R has the scaling form

$$\overline{F}(L, R) \sim L^\omega \mathcal{F}(LR^{-1/\zeta}). \quad (1.12)$$

In particular, the ‘Casimir’ term

$$\overline{f}(R) \equiv \lim_{L \rightarrow \infty} \partial_L \overline{F}(L, R) \sim R^{(\omega-1)/\zeta} \quad (1.13)$$

measures the free-energy cost per unit of t of confining a long string to a tube of width R . The exponents ζ and ω are related to the growth exponents by

$$\zeta = 1/z \quad \omega = \chi/z. \quad (1.14)$$

The scaling relation (1.6) now reads

$$\omega = 2\zeta - 1. \quad (1.15)$$

Replica methods yield the exact exponents $\zeta = 2/3$ and $\omega = 1/3$ for $d = 1$ but fail for higher dimensions.

In the superdiffusive state, the free energy acquires an anomalous dimension $-\omega < 0$. (At an ordinary critical point, the free energy is scale invariant ($\omega = 0$), which implies a set of hyperscaling relations. Such relations are no longer valid for quenched averages.)

The disorder-induced fluctuations (1.11) persist in the limit $\beta^{-1} \rightarrow 0$ —that is, in the ensemble of minimum energy paths $r_0(t)$. In the weak-coupling (high-temperature) regime for $d > 2$, thermal fluctuations dominate ($\zeta = 1/2$) and hyperscaling is preserved ($\omega = 0$). The roughening transition between these two phases takes place at a finite temperature β_c^{-1} . For $d \geq d_*$, the Gaussian exponents govern the low-temperature phase as well, albeit with possible logarithmic corrections.

1.2. Overview of this article

As emphasized already, KPZ growth defines a field theory that is *non-Lagrangian* and *non-perturbative*. This article focuses on exact properties of its local correlation functions. We mention only briefly the results of various approximation schemes. In particular, functional renormalization ([4] and references therein) and mode-coupling theory ([31, 39] and references therein) are important theoretical tools in a number of strong-coupling problems but their status in field theory is not yet fully understood.

The first part of this article describes directed strings. These systems have a fascinating spectrum of physical applications and the language of directed strings proves to be an ideal framework for addressing some of the theoretical issues of directed growth.

In section 2, we discuss directed strings in thermal equilibrium without quenched disorder. A single such string describes a free random walk and is thus generically

rough. Interactions of a single string with an external defect or mutual interactions between strings, however, can induce a localization transition destroying the long-ranged correlations of the rough state. (De-)localization phenomena are an essential feature of strings and surfaces [40]; they will appear in several contexts throughout this article. We use renormalized perturbation theory to derive the phase diagram of directed strings with short-ranged interactions and the critical behaviour at the (de-)localization transition [41–43]. The results are, of course, well known and can be derived in various other ways. The approach used here stresses that the response of the system to perturbations probes the correlations in the unperturbed, rough state. It is based on the *operator product expansion* of the local interaction fields, a familiar concept in Lagrangian field theory (see, e.g., reference [1]).

In section 3, this approach is extended to the field theory of directed strings in a random medium. In the replica formalism, a single such string is represented by a system of many strings without quenched disorder but with mutual interactions. The localized many-string state corresponds to the strong-coupling regime of the random system. Perturbative renormalization of these interactions turns out to produce the exact scaling at the roughening transition for $2 < d < 4$ but fails to describe the strong-coupling regime [18, 44]. Insight can be gained by studying several strings in a random medium with additional direct interactions. These probe the disorder-induced correlations in the scale-invariant strong-coupling regime. The temperature becomes a *dangerous irrelevant* variable at the strong-coupling fixed point; this is the field-theoretic fingerprint of quenched randomness. The direct interactions can be treated in renormalized perturbation theory about that fixed point [45, 46], assuming the existence of an operator product expansion. We find again (de-)localization transitions, which are relevant for various applications. Their critical properties are given in terms of the single-string exponents. Comparing the effect of pair interactions in the strong-coupling phase and at the roughening transition of a single string then shows that the single-string system—corresponding to the standard KPZ dynamics—has an upper critical dimension $d_{>} \leq 4$ [47, 48].

Section 4 returns to growing surfaces. The dynamical field theory of KPZ systems and its renormalization are discussed. Perturbative renormalization of the dynamic functional is compared to the string renormalization of section 3 [18], and it is shown why perturbation theory fails for the strong-coupling regime for $d > 1$. However, the scaling in this regime can be studied directly using the operator product expansion of the height field. We find that the KPZ equation can have only a discrete set of solutions distinguished by field-theoretic *anomalies* [49]. Comparing this set with numerical estimates of the exponents χ and z then gives their exact values for $d = 2$ and $d = 3$.

2. The field theory of directed strings

Ensembles of interacting directed strings describe a surprising variety of statistical systems in a unifying way. Examples are interfaces between different bulk phases in a 2D system [40], steps on crystal surfaces [50], flux lines in a type-II superconductor [51], or 1D elastic media [52]. Directed strings are also related to mathematical algorithms detecting similarities between DNA sequences [53–57].

At finite temperatures, a single string (or a collection of independent ones) would simply perform Gaussian fluctuations. It is the interactions of the strings with each other and with external objects that generate the thermodynamic complexity of these systems. Attractive forces lead to wetting transitions of interfaces, bunching transitions of steps, and depinning transitions of flux lines. All of these are transitions between a delocalized

high-temperature state with unconstrained fluctuations and a localized low-temperature state whose displacement fluctuations are constrained to a finite width ξ ; for a review, see [40]. In this and the next section, we discuss a few such systems, emphasizing their common field-theoretic aspects.

A single thermally fluctuating string is given by the partition function

$$Z = \int \mathcal{D}r \exp(-\beta S[r]) \tag{2.1}$$

with the Gaussian action

$$S[r] = \int dt \frac{1}{2} \left(\frac{d\mathbf{r}}{dt} \right)^2 \tag{2.2}$$

for the d -component displacement field $\mathbf{r}(t)$. In a finite system ($0 \leq t \leq L, 0 \leq r_1, \dots, r_d \leq R$), the universal part of the free energy has the scaling form

$$F(L, R) = \mathcal{F}(L/\beta R^2). \tag{2.3}$$

This defines in particular the Casimir amplitude

$$\mathcal{C}(R) \equiv \beta^2 R^2 \lim_{L \rightarrow \infty} \partial_L F(L, R) \tag{2.4}$$

measuring the scaled free-energy cost per unit of t of confining a long string to a tube of width R . It depends only on the boundary conditions in the transverse direction. For periodic boundary conditions, $\mathcal{C} = 0$.

The displacement field $\mathbf{r}(t)$ has the negative scaling dimension $-\zeta_0 = -1/2$. Its two-point function

$$\langle \mathbf{r}(t_1) \cdot \mathbf{r}(t_2) \rangle = \int d\omega \frac{e^{i\omega(t_1-t_2)}}{\omega^2} \tag{2.5}$$

requires an infrared regularization by appropriate boundary conditions. It is the difference correlation function

$$\langle (\mathbf{r}(t_1) - \mathbf{r}(t_2))^2 \rangle = -2\langle \mathbf{r}(t_1)\mathbf{r}(t_2) \rangle + \langle \mathbf{r}^2(t_1) \rangle + \langle \mathbf{r}^2(t_2) \rangle \sim |t_1 - t_2|^{2\zeta_0} \tag{2.6}$$

that remains well defined in the thermodynamic limit $L, R \rightarrow \infty$ and becomes scale invariant. The exponent ζ_0 is called the thermal roughness exponent.

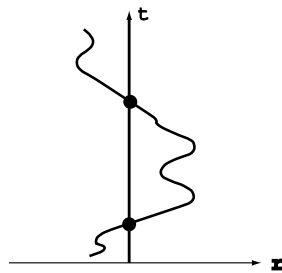


Figure 3. A thermally fluctuating directed string $\mathbf{r}(t)$ and a rigid linear defect at $\mathbf{r} = 0$. Contact interactions between these objects are described by the local scaling field $\Phi(t)$.

Consider now a directed string interacting with a rigid linear defect at $\mathbf{r} = 0$ as shown in figure 3. If the interaction decays on the microscopic scale $|\mathbf{r}| \sim a$, the system has the action

$$S[r] = \int dt \left(\frac{1}{2} \left(\frac{d\mathbf{r}}{dt} \right)^2 + g_0 \Phi(t) \right) \tag{2.7}$$

in the continuum limit $a \rightarrow 0$. The local interaction of the string with the defect is proportional to the contact field $\Phi(t) \equiv \delta(\mathbf{r}(t))$ of canonical scaling dimension $x_0 = d\zeta_0$. The conjugate coupling constant g_0 has the dimension $y_0 = 1 - x_0$ with t as the basic scale.

Of course, this system can be treated exactly, for example by solving the imaginary-time Schrödinger equation

$$\beta^{-1} \partial_t Z = \frac{\beta^{-2}}{2} \nabla^2 Z + g_0 \delta(\mathbf{r}) Z \tag{2.8}$$

for the wave function (1.9); see [58] in the context of directed strings. Here we discuss a different method of solution [41–43] that can be generalized to problems with quenched disorder. For the purposes of this section, it is convenient to set $\beta = 1$, which amounts to the substitution $t \rightarrow \beta^{-1}t$ in the action (2.7).

2.1. Correlation functions and the operator product expansion

The perturbative analysis of the interaction in (2.7) is based on the correlation functions $\langle \Phi(t_1) \cdots \Phi(t_N) \rangle$ in the unperturbed state, which can be calculated explicitly. We take each component of the displacement vector to be compactified on a circle of circumference R . The scale R also serves to generate the renormalization group flow defined below. With this regularization, longitudinal translation invariance emerges for ‘bulk’ values $0 \ll t_1, \dots, t_N \ll L$ in the limit $L \rightarrow \infty$ independently of the boundary conditions at $t = 0$ and $t = L$.

The translation-invariant one-point function

$$\langle \Phi(t) \rangle \equiv \langle \Phi \rangle = R^{-x_0/\zeta_0} \tag{2.9}$$

is simply the probability (density) of finding the fluctuating string $\mathbf{r}(t)$ at the origin $\mathbf{r} = 0$ for a given t . Similarly, the N -point function $\langle \Phi(t_1) \cdots \Phi(t_N) \rangle$ is the joint probability of the configurations with N intersections of the origin at given values t_1, \dots, t_N .

These correlation functions develop singularities as some of the points approach each other. For example, the joint probability of intersecting the origin $\mathbf{r} = 0$ both at t and at t' equals the single-event probability (2.9) multiplied by the probability of return to the origin after a ‘time’ $|t - t'|$, which becomes singular as $t' \rightarrow t$:

$$\langle \Phi(t)\Phi(t') \rangle = C_0 |t - t'|^{-x_0} \langle \Phi(t) \rangle + \dots \tag{2.10}$$

with $C_0 = (2\pi)^{-x_0}$.

The structure of this singularity and the coefficient C_0 are local properties: they appear in any (connected) N -point function as two of the arguments t_i, t_j approach each other, independently of the other points remaining at a finite distance and of the infrared regularization. This can be expressed by the field relation [41]

$$\Phi(t)\Phi(t') = C_0 |t - t'|^{-x_0} \Phi(t) + \dots \tag{2.11}$$

illustrated in figure 4. It is called an operator product expansion (a familiar concept in field theory; see, e.g., reference [1]). The dots denote less singular terms involving gradient fields. Such terms are generated, for example, if the r.h.s. of (2.11) is expressed in terms of $\Phi(t') = \Phi(t) + (t' - t)\Phi'(t) + \dots$, which leaves the leading singularity invariant.

2.2. Renormalization

It is convenient to set up the perturbation theory for the Casimir amplitude (2.4). Since \mathcal{C} is a dimensionless number, the contribution of the interaction

$$\Delta C(u_0) \equiv \mathcal{C}(g_0, R) - \mathcal{C}(0, R) \tag{2.12}$$

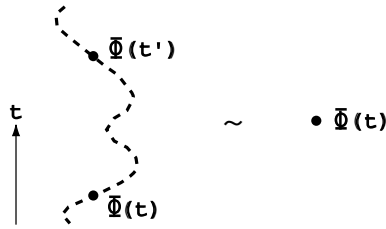


Figure 4. The operator product expansion of contact fields for a thermally fluctuating string. The short-distance asymptotics of the pair of fields $\Phi(t)$ and $\Phi(t')$ is given by the single field $\Phi(t)$ multiplied by a singular prefactor. The dashed line indicates the string configurations generating the singularity $|t - t'|^{-x_0}$.

depends only on the dimensionless coupling constant

$$u_0 \equiv g_0 R^{y_0/\zeta_0}. \quad (2.13)$$

The perturbation expansion

$$\Delta\mathcal{C}(u_0) = -R^2 \sum_{N=1}^{\infty} \frac{(-g_0)^N}{N!} \int dt_2 \cdots dt_N \langle \Phi(t_1) \cdots \Phi(t_N) \rangle^c \quad (2.14)$$

contains integrals over connected correlation functions of the contact field in the Gaussian theory ($g_0 = 0$). Hence, the singularities of the operator product expansion (2.11) lead to poles in (2.14). Inserting (2.9) and (2.11) into (2.14), we obtain

$$\Delta\mathcal{C}(u_0) = R^{x_0/\zeta_0} \langle \Phi \rangle \left(u_0 - \frac{C_0}{y_0} u_0^2 \right) + \mathcal{O}(y_0^0 u_0^2, u_0^3). \quad (2.15)$$

The same type of singularity (with different combinatoric factors) occurs in the expansion of correlation functions $\langle \Phi(t_1) \cdots \Phi(t_N) \rangle(u_0)$. For example,

$$\begin{aligned} \langle \Phi \rangle(u_0, R) &= \sum_{N=0}^{\infty} \frac{(-g_0)^N}{N!} \int dt_1 \cdots dt_N \langle \Phi(t) \Phi(t_1) \cdots \Phi(t_N) \rangle^c \\ &= \langle \Phi \rangle \left(1 - \frac{2C_0}{y_0} u_0 \right) + \mathcal{O}(y_0^0 u_0, u_0^2). \end{aligned} \quad (2.16)$$

Perturbative renormalization consists in absorbing the singularities of the ‘bare’ series (2.14) and (2.16) into new variables u_P and Φ_P defined order by order. (We use the subscript P to distinguish perturbatively defined couplings and fields from their non-perturbatively renormalized counterparts. This distinction is not necessary in the present context but will become crucial below.) To leading (one-loop) order, the coupling constant renormalization can be read off directly from equation (2.15). Defining

$$u_P \equiv \mathcal{Z}_P u_0 \quad (2.17)$$

with

$$\mathcal{Z}_P(u_P) = 1 - \frac{C_0}{y_0} u_P + \mathcal{O}(y_0^0 u_P, u_P^2) \quad (2.18)$$

the Casimir amplitude as function of u_P becomes finite to order u_P^2 :

$$\Delta\mathcal{C}(u_P) = R^{x_0/\zeta_0} \langle \Phi \rangle u_P + \mathcal{O}(y_0^0 u_P^2, u_P^3). \quad (2.19)$$

The coupling constant renormalization (2.18) implies a renormalization of the conjugate field:

$$\Phi_P(t) \equiv \tilde{\mathcal{Z}}_P \Phi(t) \quad (2.20)$$

with

$$\tilde{\mathcal{Z}}_P(u_P) = \frac{du_0}{du_P} = 1 + \frac{2C_0}{y_0}u_P + \mathcal{O}(y_0^0 u_P, u_P^2). \quad (2.21)$$

This also renders the correlation functions $\langle \Phi_P(t_1) \cdots \Phi_P(t_N) \rangle(u_P)$ finite. The scale dependence of u_P is governed by the flow equation

$$\dot{u}_P \equiv \zeta_0 R \partial_R u_P = \frac{y_0 u_P}{1 - u_P (d/du_P) \log \tilde{\mathcal{Z}}_P}. \quad (2.22)$$

Using (2.18), we obtain

$$\dot{u}_P = y_0 u_P - C_0 u_P^2 + \mathcal{O}(y_0 u_P^2, u_P^3). \quad (2.23)$$

Hence, the one-loop \mathcal{Z} -factors and the resulting flow equation are entirely determined by the constants y_0 and C_0 encoding local properties of the unperturbed theory.

For this particular system, the one-loop equations turn out to be very powerful because the pole at order u_0^2 is the only primitive singularity for $y_0 \rightarrow 0$ in the bare perturbation series. Hence, the theory is *one-loop renormalizable* [59, 60, 18]: it can be described by the flow equation

$$\dot{u}_P = y_0 u_P - C_0 u_P^2 \quad (2.24)$$

terminating at second order. This property leads to exact results for local observables of the perturbed theory. In the appendix, it is derived for the more general many-string system of section 3.2.

Of course, the form (2.24) of the flow equation is not unique. It depends on the infrared regularization of the bare perturbation series and on the renormalization conditions defining the coupling constant u_P . Changing either amounts to finite reparametrizations of u_P . Linear reparametrizations change the coefficient of u_P^2 in (2.24), while non-linear reparametrizations introduce higher-order terms (see the discussion in the appendix). However, local observables of the perturbed theory are ‘gauge invariant’; i.e., independent of these choices. They can be computed exactly from (2.24) and the associated \mathcal{Z} -factors (A.13). The simplest such observable is the anomalous dimension

$$x^* = x_0 - \dot{u}_P \left. \frac{d}{du_P} \log \tilde{\mathcal{Z}}_P(u_P) \right|_{u_P^*} = 1 + y_0. \quad (2.25)$$

It governs the correlation functions of the contact field at the non-trivial fixed point u_P^* of the flow equation; for example,

$$\langle \Phi(t) \rangle \sim R^{-x^*/\zeta_0} \quad (2.26)$$

and

$$\langle \Phi(t)\Phi(t') \rangle \sim |t - t'|^{-x^*} \langle \Phi(t) \rangle \quad (2.27)$$

for $|t - t'| \ll R^2$. By simple scaling arguments, it follows from (2.26) that the normalized string density

$$P(|\mathbf{r}'|) \equiv \langle \delta(\mathbf{r}(t) - \mathbf{r}') \rangle / \int d\mathbf{r} \langle \delta(\mathbf{r}(t) - \mathbf{r}') \rangle \quad (2.28)$$

has the singularity

$$P(r) \sim r^\theta R^{-d-\theta} \quad \text{for } r \ll R \quad (2.29)$$

with

$$\theta = -\frac{x^*}{\zeta} - d = 4y_0 = 2(2 - d). \quad (2.30)$$

Of course, the exponent θ can be obtained in a simpler way. The Schrödinger equation (2.8) has the singular ground-state wave function $Z \sim r^{2-d}$, and $P \sim Z^2$.

2.3. Results and discussion

For $d < 2$, the Gaussian fixed point $u_P = 0$ is unstable under the flow (2.24) and governs the (de-)localization transition. Close to the transition, the localization width has the singularity

$$\xi \sim (-g_0)^{-\zeta_0/y_0} \quad (g_0 < 0). \tag{2.31}$$

The fixed point u^* is stable and determines the asymptotic scaling with repulsive contact interactions in the limit $R \rightarrow \infty$ or $g_0 \rightarrow \infty$. The string density $P(r)$ then has a long-ranged depletion given by (2.29) with $\theta > 0$.

At the borderline dimension $d = 2$, where the two fixed points coalesce, the theory is asymptotically free with

$$\xi \sim \exp(-C_0 \zeta_0/g_0) \quad (g_0 < 0). \tag{2.32}$$

For $2 < d < 4$, the transition is governed by the non-trivial fixed point with

$$\xi \sim (g_c - g_0)^{-\zeta_0/y^*} \quad (g_0 < g_c) \tag{2.33}$$

and $y^* = 1 - x^* = -y_0$. This fixed point now has a negative value of θ , describing a divergence of the string density $P(r)$ for $r \rightarrow 0$ due to the attractive interaction.

It is obvious that the same scaling occurs in a number of related systems. For a directed string $(r_1 > 0, r_2, \dots, r_d)(t)$ confined to half space, the term $g_0 \delta(r_1)$ describes a short-ranged interaction with the boundary of the system. The scaling of the string close to the boundary is described by the above two fixed points for $d = 1$ with the transition point shifted to a value $g_c < 0$ and the fluctuations parallel to the boundary decoupled. Similarly, a single directed string interacting with a linear defect is equivalent to the two-string system

$$Z = \int dr_1 dr_2 \exp(-\beta S[r_1, r_2])$$

with the action

$$S[r_1, r_2] = \int dt \left(\frac{1}{2} \left(\frac{dr_1}{dt} \right)^2 + \frac{1}{2} \left(\frac{dr_2}{dt} \right)^2 + g_0 \Psi(t) \right) \tag{2.34}$$

containing pair interactions $\Psi(t) \equiv \delta(r_1(t) - r_2(t))$. The centre-of-mass fluctuations are decoupled, and (2.28) is the pair density with $r(t) = r_1(t) - r_2(t)$. For $d = 1$, Gaussian strings with contact repulsions are known to behave asymptotically like free fermions [61], and (2.30) then gives the correct scaling $P(r) \sim r^2$ of the pair density imposed by the antisymmetry of the fermionic wave function.

Leaving aside these specifics of Gaussian strings, the qualitative features of the phase diagram are seen to rest on two properties of the local interaction field $\Phi(t)$: its scaling dimension depends on d in a continuous way and it obeys an operator product expansion with a self-coupling term (2.11). These properties are found to be preserved for directed strings in a random medium despite the lack of a local action.

It turns out that the renormalization discussed in this section is also applicable to temperature-driven transitions in systems of many directed strings. An example of current experimental interest is *vicinal surfaces*, i.e., crystal surfaces miscut at a small angle with respect to one of the symmetry planes. A vicinal surface can be regarded as an ensemble of terraces and steps [50]. The steps are non-crossing (fermionic) directed strings. They are coupled by mutual forces that turn out to have a short-ranged attractive and a long-ranged repulsive part [62]. Typical step configurations are shown in figure 5.

At high temperatures, the ensemble of steps is homogeneous. Below a faceting temperature (that depends on the step density), the steps are found to form local bundles. Hence, the surface splits up into domains of an increased and temperature-dependent step

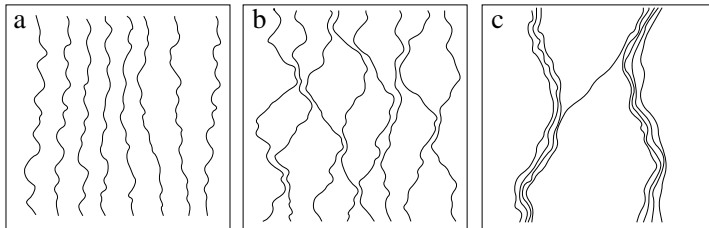


Figure 5. (De-)localization in a system of many strings. In this example, the strings are steps on a crystal surface coupled by inverse-square and short-ranged forces. Typical step configurations at different temperatures are the following. (a) Well above the critical temperature T_c , the steps are dominated by the no-crossing constraint and the long-ranged repulsion. Hence, they are well separated from each other with relatively small fluctuations. (b) In the critical regime near T_c , the probability of a step being close to one of its neighbours is substantially enhanced. This is accompanied by increased step fluctuations and a broader distribution of terrace widths. (c) Below the faceting temperature, the steps form local bundles. On average, the distance between two neighbouring bundles is larger than the width of an individual bundle. The fluctuations of these ‘composite’ steps are smaller than those of individual steps.

density alternating with step-free facets [63]. A critical regime containing the *faceting transition* (the analogue of the (de-)localization transition of two strings) separates the high- and low-temperature regimes. In the renormalization group, one still finds a pair of fixed points linked by an exact one-loop renormalization group for the strength of the contact interaction. These fixed points determine the faceting transition and the high-temperature regime, respectively [64]. The long-ranged forces influence the universal features (e.g., the scaling of the contact field) of both fixed points in a characteristic way. This determines, for example, the distribution of terrace widths and the density of steps in a bundle. The theoretical results compare favourably with recent experiments on Si surfaces [63, 65].

The thermodynamic complexity of this many-string system is due to an interplay of attractive interactions, Fermi statistics, and repulsive forces. In the next section, we shall discuss the much simpler case of bosonic strings (i.e., strings allowed to intersect) with contact attractions only. For $d = 1$, the latter will collapse to a bound state at any temperature. However, qualitatively different behaviour emerges in the formal limit of vanishing number of strings. This limit turns out to describe a single string in a random medium.

3. Directed strings in a random medium

In this section, interactions between strings play a double role. On the one hand, a single string in a quenched random medium can formally be represented as a system of p strings without disorder but with mutual interactions, in the limit $p \rightarrow 0$ [37]. This well-known replica formalism turns out to be a convenient basis for the perturbative renormalization of the random system [18].

On the other hand, additional interactions are important in many applications of directed strings in random media. An example is the physics of superconductors [51, 68–70]. A type-II superconductor in a magnetic field h above a critical strength h_{c1} contains magnetic flux lines at a density that depends on h . The lines are directed parallel to the magnetic field. Their thermally activated transverse fluctuations dissipate energy at the expense of the supercurrent. The superconductor may be doped with point impurities, linear or planar

defects designed to suppress these fluctuations by localizing the flux lines. Linear defects are generated, for example, by irradiating the material with heavy ions [71, 72].

As the external field approaches the critical value h_{c1} , the ensemble of flux lines becomes dilute. It is then useful to study the approximation of a single flux line interacting with a single columnar defect in the presence of point impurities [73–76, 45]; see figure 6(a). The next step is to consider pair interactions in a dilute ensemble of lines as shown in figure 6(b) [77–80, 46].

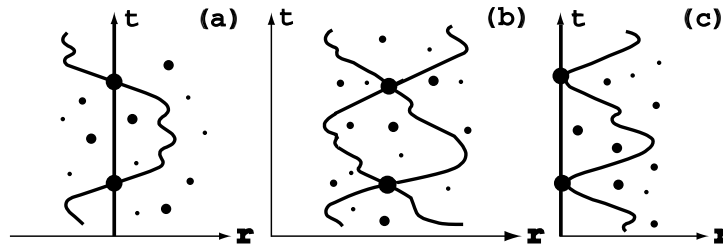


Figure 6. Directed strings in a disordered medium with additional contact interactions. (a) A string and a rigid linear defect. (b) Two strings with mutual interactions. (c) A string and a wall.

The interaction of strings with the boundaries of the system (figure 6(c)) can be discussed on a similar theoretical footing. The particular case of one transverse dimension, where the string becomes an interface of the system, has been of interest as a simple model for wetting in a random medium [37]. The interaction of a string with a linear defect is also relevant in the context of DNA pattern recognition [53–57]. Two related DNA sequences in different organisms have mutual correlations inherited from their common ancestor in the evolution process. The algorithmic detection of these correlations turns out to correspond to a localized state of a string.

It is not surprising that a random medium, by changing the displacement statistics of a single string, also modifies its direct interactions with other strings and with external objects. In the renormalization group for these transitions, quenched impurities enter in a characteristic way: the strong-coupling fixed point has a dangerous irrelevant coupling constant that alters the scaling properties of the direct interactions [45]. Consequently, the (de-)localization transitions differ from those in pure systems. In turn, the response to such interactions becomes a theoretical tool for studying the correlations at the strong-coupling fixed point. This is used at the end of this section to show that the single-string system has an upper critical dimension less than or equal to four [47].

3.1. Replica perturbation theory

A medium with quenched pointlike impurities exerts a local random potential $\eta(\mathbf{r}, t)$ on a directed string. For a given configuration of the impurities, the partition function of the string is

$$Z[\eta] = \int \mathcal{D}r \exp(-\beta S[\mathbf{r}, \eta]) \quad (3.1)$$

with the action (1.10):

$$S[\mathbf{r}, \eta] = \int dt \left(\frac{1}{2} \left(\frac{d\mathbf{r}}{dt} \right)^2 + \eta(\mathbf{r}(t), t) \right) \quad (3.2)$$

where λ has been set to 1. We take the local potential variables to have the Gaussian distribution given by (1.2) and compute average quantities like the free energy

$$\bar{F} = -\beta^{-1} \int \mathcal{D}\eta \exp\left(-\int dt d\mathbf{r} \frac{1}{2\sigma^2} \eta^2(t, \mathbf{r})\right) \log Z[\eta]. \quad (3.3)$$

At first sight, this system looks quite different from those of the previous section. However, we can write $\log Z[\eta]$ as a partition function of p independent strings labelled by the index α :

$$\log Z[\eta] = \lim_{p \rightarrow 0} \frac{1}{p} \left(\prod_{\alpha=1}^p Z^{(\alpha)}[\eta] - 1 \right). \quad (3.4)$$

In the replicated system, the integration over the η variables can be performed [37]. This gives

$$\bar{F} = \lim_{p \rightarrow 0} \frac{1}{p} F_p \quad (3.5)$$

with

$$F_p = -\beta^{-1} \log \int \mathcal{D}\mathbf{r}_1 \cdots \mathcal{D}\mathbf{r}_p \exp(-\beta S[\mathbf{r}_1, \dots, \mathbf{r}_p]) \quad (3.6)$$

and the action

$$S[\mathbf{r}_1, \dots, \mathbf{r}_p] = \int dt \left(\sum_{\alpha=1}^p \frac{1}{2} \left(\frac{d\mathbf{r}_\alpha}{dt} \right)^2 - \beta \sigma^2 \sum_{\alpha < \beta} \Phi_{\alpha\beta}(t) \right). \quad (3.7)$$

The coupling of the original string $\mathbf{r}(t)$ to the random medium now appears as a contact attraction $\Phi_{\alpha\beta}(t) \equiv \delta(\mathbf{r}_\alpha(t) - \mathbf{r}_\beta(t))$ between the replicas (i.e., phantom copies) $\mathbf{r}_1(t), \dots, \mathbf{r}_p(t)$. The free energy of the replicated system is related to the cumulant expansion of the random free energy [37]:

$$F_p = \sum_{k=1}^{\infty} \frac{p^k}{k!} F^k. \quad (3.8)$$

The physical properties of this system strongly depend on p . For $p > 1$, the attractive interaction *reduces* the fluctuations of the strings. A single string ($p = 1$) undergoes no interaction. Randomness *enhances* the string fluctuations, and this is naturally associated with values $p < 1$. The existence of the random limit $p \rightarrow 0$ is not clear *a priori*. It can be established for $d = 1$, where the replica system is exactly solvable (see section 3.2). For higher dimensions, the replica interaction can still be treated in perturbation theory.

For arbitrary values of p , the path integral in equation (3.6) can be rewritten in second quantization [18]:

$$Z = \int \mathcal{D}\phi \mathcal{D}\bar{\phi} \exp \left[-\beta \int dt d\mathbf{r} \left(\bar{\phi} \left(\partial_t - \frac{1}{2\beta} \nabla^2 \right) \phi - \beta \sigma^2 \bar{\phi}^2 \phi^2 \right) \right]. \quad (3.9)$$

The contact attraction is described by the (normal-ordered) vertex $\bar{\phi}^2 \phi^2$. Since this interaction conserves the number of strings, the dependence of (3.9) on p is contained entirely in the boundary conditions at early and late values of t . Hence, the boundary conditions are important for obtaining the replica limit $p \rightarrow 0$.

The representation (3.9) is a convenient framework for perturbation theory [18]. We now label the parameters β_0^{-1}, σ_0^2 , the free energy and all longitudinal lengths with the

subscript 0 to distinguish them from their renormalized counterparts introduced below. In the appendix, the renormalization is carried out for the disorder-averaged Casimir amplitude

$$\bar{C} = \beta_0^2 R^2 \bar{f}_0(R) \tag{3.10}$$

defined by equation (1.13). The disorder-induced part

$$\Delta\bar{C}(\sigma_0^2, \beta_0^{-1}, R) \equiv \bar{C}(\sigma_0^2, \beta_0^{-1}, R) - \bar{C}(0, \beta_0^{-1}, R) \tag{3.11}$$

can be expanded in powers of the dimensionless coupling constant $u_0 = g_0 R^{y_0/\zeta_0}$, where

$$g_0 = -\beta_0^3 \sigma_0^2 \tag{3.12}$$

and $y_0 = (2 - d)/2$. Due to proliferation of replica indices, the perturbation series is more complicated than its analogue in the previous section [44]. However, as shown in the appendix, it is still one-loop renormalizable: the Casimir amplitude (3.10) is a regular function of the coupling constant $u_P = \mathcal{Z}_P u_0$ defined by (A.13):

$$\beta^2 \Delta\bar{C}(u_P) = -\frac{1}{4} u_P + O(y_0 u_P, u_P^2). \tag{3.13}$$

An immediate consequence of the one-loop renormalizability is that the strong-coupling regime is beyond the reach of the loopwise perturbation expansion (A.3) since the flow equation (2.24) does not have a stable fixed point at negative values of u_P [18]. (The fixed point $u_P^* = y_0/C_0 > 0$ for $d < 2$ is unphysical in this context since a repulsive interaction between replicas translates into a purely imaginary random potential.) We come back to this failure of perturbation theory in section 4.2.

The fixed point $u_P^* < 0$ for $d > 2$ is to be identified with the roughening transition. At this fixed point, the Casimir amplitude (3.10) takes a finite positive value without any explicit dependence on R :

$$\bar{C}^* = -\frac{1}{4} \frac{y_0}{C_0} + O(y_0^2). \tag{3.14}$$

The scaling properties at the transition can hence be obtained exactly from the one-loop renormalization group [18, 44]. For example, the displacement fluctuations are still only diffusive:

$$\zeta^* = 1/2 \quad \omega^* = 0. \tag{3.15}$$

This follows by comparing (3.14) with the scaling $\bar{C} \sim R^{2\omega/\zeta}$ at a generic fixed point given by (1.13). Other exponents do depend on d . Conjugate to σ_0^2 is the local field

$$\Phi_\eta(t_0) \equiv \int d\mathbf{r}' \eta(\mathbf{r}', t_0) \delta(\mathbf{r}(t_0) - \mathbf{r}') \tag{3.16}$$

which encodes the random potential evaluated along the string [47]. Small variations of σ_0^2 (i.e., of u_P) are a relevant perturbation at the roughening transition. The dimension

$$y^* = \frac{d-2}{2} \tag{3.17}$$

is given by the eigenvalue of the beta function at the fixed point u_P^* . The dimension of Φ_η is therefore $x^* = (4 - d)/2$. In the action (3.7), this field becomes the replica pair field $\Phi_{\alpha\beta}(t)$. The same dimension x^* then follows from (2.25) with the field renormalization (A.13). One may also define the pair contact field $\Psi(t) \equiv \delta(\mathbf{r}_1(t) - \mathbf{r}_2(t))$ of two real copies, i.e., two independent strings $\mathbf{r}_1(t)$ and $\mathbf{r}_2(t)$ in the same random potential. It can be shown that this field and its conjugate coupling constant also have dimensions x^* and y^* , respectively.

The perturbative calculation can only be trusted for $d < 4$. The fact that x^* would become negative for $d > 4$ is clearly unphysical. Moreover, physical quantities become singular as d approaches 4; for example, $\mathcal{C}^* \sim \sqrt{4-d}$ [44]. This shows that $d = 4$ is a singular dimension for the roughening transition and ties in with the existence of an upper critical dimension $d_{\geq} \leq 4$ of the strong-coupling phase.

3.2. The strong-coupling regime

In the strong-coupling regime (i.e. for low temperatures or large disorder amplitudes), the string has the disorder-induced fluctuations

$$\overline{(\mathbf{r}(t) - \mathbf{r}(t'))^2} \sim |t - t'|^{2\zeta} \tag{3.18}$$

leading to anomalous scaling of the confinement free energy (1.13):

$$\overline{f}(R) \sim R^{(\omega-1)/\zeta} \tag{3.19}$$

(see references [36, 38]). The exponents satisfy the scaling relation (1.15). Superdiffusive scaling ($\omega = 2\zeta - 1 > 0$) is believed to persist up to an upper critical dimension d_{\geq} (see section 3.6).

In $d = 1$, the exponents can be obtained exactly from the replica approach [37]. The system of p strings is always in a bound state for integer $p > 1$. The binding energy in a system of infinite width R ,

$$E_p = \lim_{L \rightarrow \infty} \partial_L (F_p(\beta_0, \sigma_0^2, L) - F_p(\beta_0, 0, L)) \tag{3.20}$$

can be computed by Bethe *ansatz* methods; one finds

$$E_p \sim p + O(p^3).$$

Analytically continued to $p = 0$ and inserted in (3.8), this gives $\overline{F}^{3^c} \sim L$; hence $\omega = 1/3$, and $\chi = 2/3$ by (1.15).

In higher dimensions, the strings form a bound state only for $\sigma_0^2 > \sigma_{0c}^2$. If we assume that E_p is still analytic in p and has the form

$$E_p \sim p + O(p^{k_0+1}) \quad (k_0 = 2, 3, \dots)$$

the same argument yields

$$\omega = \frac{1}{k_0 + 1} \tag{3.21}$$

(see the discussion in [66, 67]). The exponents of the random system are indeed quantized, as will be discussed in the context of the Kardar–Parisi–Zhang equation in section 4. The quantization condition (4.1) is consistent with (3.21).

In the continuum theory (3.1), the large-distance scaling (3.18) and (3.19) is reached in a crossover from diffusive behaviour on smaller scales. The crossover has characteristic longitudinal and transverse scales \tilde{t}_0 and \tilde{r} beyond which the disorder-induced fluctuations dominate over the thermal fluctuations. The dependence of these scales on the effective coupling (3.12), namely

$$\tilde{r}^2 = \beta_0^{-1} \tilde{t}_0 = \begin{cases} (-g_0)^{-1/y_0} & (d < 2, g_0 < 0) \\ \exp(-C_0/g_0) & (d = 2, g_0 < 0) \\ (g_c - g_0)^{-1/y^*} & (2 < d < 4, g_0 < g_c) \end{cases} \tag{3.22}$$

with $y_0 = 2/(2 - d) = -y^*$, can be obtained from the replica action (3.7); see equations (2.31)–(2.33). The string displacement and the confinement free energy have the form

$$\overline{\langle (\mathbf{r}(t_0) - \mathbf{r}(t'_0))^2 \rangle} \sim \beta_0^{-1} t_0 \tilde{\mathcal{R}}(t_0/\tilde{t}_0) \tag{3.23}$$

and

$$\bar{f}_0 \sim \beta_0^{-2} R^{-2} \tilde{\mathcal{F}}(R/\bar{r}) \tag{3.24}$$

with scaling functions that are finite in the short-distance limits $t_0 \ll \tilde{t}_0$ and $R \ll \xi$, respectively. In the opposite limit, comparison with (3.18) and (3.19) exhibits the singular dependence on the bare parameters β_0^{-1} and σ_0^2 contained in the scaling functions:

$$\overline{\langle (\mathbf{r}(t_0) - \mathbf{r}(t'_0))^2 \rangle} \sim \beta_0^{-2\zeta} \tilde{t}_0^{-2\omega} |t_0 - t'_0|^{2\zeta} \tag{3.25}$$

and

$$\bar{f}_0 \sim \beta_0^{-2} \tilde{r}^{-1} R^{-1}. \tag{3.26}$$

These singularities can be absorbed into the definition of the renormalized quantities

$$t = (\beta/\beta_0)t_0 \quad \bar{f} = (\beta_0/\beta)\bar{f}_0 \tag{3.27}$$

written in terms of the renormalized temperature

$$\beta^{-1} = \tilde{r}^{\omega/\zeta} = \tilde{t}^\omega \tag{3.28}$$

(see the discussion in [45]). The renormalized displacement function and confinement free energy remain finite in the continuum limit $\tilde{r} \rightarrow 0$ (i.e. for $\beta_0^{-1} \rightarrow 0$ or $\sigma_0^2 \rightarrow \infty$), as follows from inserting (3.27) and (3.28) into (3.25) and (3.26).

The existence of a zero-temperature continuum limit is crucial if the ensemble of ground states generated by the quenched disorder is to have universal features. According to equation (3.28), the renormalized temperature β^{-1} is an irrelevant coupling constant of dimension $-\omega$. This is why the renormalized theory may be called a zero-temperature fixed point. It will be shown below that β^{-1} is a *dangerous* irrelevant variable which modifies the correlations of other fields in a characteristic way [45].

3.3. A string and a linear defect

A single string coupled to a random medium and a linear defect has the partition function (3.1) with the action

$$S[\mathbf{r}, \eta] = \int dt \left(\frac{1}{2} \left(\frac{d\mathbf{r}}{dt} \right)^2 + \eta(\mathbf{r}(t), t) + g\Phi(t) \right) \tag{3.29}$$

containing the contact field $\Phi(t) \equiv \delta(\mathbf{r}(t))$. The string configurations are determined by a competition between two kinds of interaction. Point defects roughen the string and make its displacement fluctuations superdiffusive. An attractive extended defect, on the other hand, suppresses these excursions and, if it is sufficiently strong, localizes the string to within a finite transverse distance ξ . As in section 2, the two regimes are separated by a second-order phase transition where the localization length ξ diverges. In contrast to temperature-driven transitions, it involves the competition of two different configuration energies rather than energy and entropy. Hence, the transition persists in the zero-temperature limit.

The properties of this zero-temperature phase transition have been controversial [73–76, 45]. Following the treatment of [45], we expand the defect contribution

$$\Delta\bar{\mathcal{C}}(g, R) \equiv \bar{\mathcal{C}}(g, R) - \bar{\mathcal{C}}(0, R) \tag{3.30}$$

to the zero-temperature Casimir amplitude

$$\bar{C} \equiv R^{(1-\omega)/\zeta} \bar{f}(R) \quad (3.31)$$

about the point $g = 0$ given by the strong-coupling continuum theory. This leads to a perturbation series formally analogous to (2.14):

$$\Delta \bar{C}(g, R) = -\beta^{-1} R^{(1-\omega)/\zeta} \sum_{N=1}^{\infty} \frac{(-\beta g)^N}{N!} \int dt_2 \cdots dt_N \overline{\langle \Phi(t_1) \cdots \Phi(t_N) \rangle^c}. \quad (3.32)$$

Of course, the perturbation series cannot be evaluated explicitly since the multipoint correlation functions of the contact field at the zero-temperature fixed point are not known exactly. However, one can still write down the one-point function

$$\overline{\langle \Phi(t) \rangle} \equiv \overline{\langle \Phi \rangle} = R^{-x/\zeta} \quad (3.33)$$

(with $x = d\zeta$) and establish the short-distance structure of the higher connected correlation functions.

Consider first the displacement function (1.11). It has the low-temperature expansion

$$\overline{\langle (\mathbf{r}(t) - \mathbf{r}(t'))^2 \rangle} = |t - t'|^{2\zeta} + \beta^{-1} |t - t'|^{2\zeta - \omega} + \cdots \quad (3.34)$$

assuming analyticity of the crossover scaling form (3.23) in the scaling variable β^{-1} . Hence at zero temperature, equation (1.11) equals its thermally disconnected part $\overline{\langle \mathbf{r}(t) - \mathbf{r}(t') \rangle^2}$. The connected part can be shown to equal that of the Gaussian theory [38]:

$$\overline{\langle (\mathbf{r}(t) - \mathbf{r}(t'))^2 \rangle^c} \sim \beta^{-1} |t - t'|. \quad (3.35)$$

It appears as the leading correction to the scaling in (3.34).

In analogy to (2.10), the two-point function $\overline{\langle \Phi(t) \Phi(t') \rangle}$ is assumed to factorize for $|t - t'| \ll R^{1/\zeta}$ into the one-point function $\overline{\langle \Phi(t) \rangle}$ multiplied by the R -independent probability of returning to the origin, which is proportional to the inverse r.m.s. displacement given by (3.34):

$$\overline{\langle \Phi(t) \Phi(t') \rangle} \sim |t - t'|^{-x} (1 - \beta^{-1} d^{-1} |t - t'|^{-\omega} + \cdots) \overline{\langle \Phi(t) \rangle}. \quad (3.36)$$

Again the leading singularity is due to sample-to-sample fluctuations of the minimal-energy paths, while the correction term is due to thermal fluctuations around these paths. At zero temperature, the field $\Phi(t)$ can be replaced by its thermal expectation value $\langle \Phi(t) \rangle$; hence $\overline{\langle \Phi(t) \Phi(t') \rangle}$ equals its thermally disconnected part $\overline{\langle \Phi(t) \rangle \langle \Phi(t') \rangle}$ and the connected part $\overline{\langle \Phi(t) \Phi(t') \rangle^c}$ vanishes, just as the connected displacement function (3.35) does. The subleading term in (3.36) is the sum of $\overline{\langle \Phi(t) \Phi(t') \rangle^c}$ and a temperature-dependent correction to $\overline{\langle \Phi(t) \rangle \langle \Phi(t') \rangle}$. An analogous argument applies to the singularities in any correlation function $\overline{\langle \cdots \Phi(t) \Phi(t') \cdots \rangle}$ as $|t - t'| \rightarrow 0$. This leads to the operator product expansion

$$\Phi(t) \Phi(t') \sim C \beta^{-1} |t - t'|^{-x-\omega} \Phi(t) \quad (3.37)$$

with a constant $C > 0$. Defining the contact field $\Phi(\mathbf{r}', t) \equiv \delta(\mathbf{r}(t) - \mathbf{r}')$, equation (3.37) can be generalized to the spatio-temporal operator product expansion

$$\Phi(\mathbf{r}, t) \Phi(\mathbf{r}', t') \sim C \beta^{-1} |t - t'|^{-x-\omega} \mathcal{H} \left(\frac{v|t - t'|}{|\mathbf{r} - \mathbf{r}'|^\zeta} \right) \Phi(\mathbf{r}, t) \quad (3.38)$$

producing a spatial singularity of the form

$$\Phi(\mathbf{r}, t) \Phi(\mathbf{r}', t) \sim \beta^{-1} |\mathbf{r} - \mathbf{r}'|^{-d-\omega/\zeta} \Phi(\mathbf{r}, t). \quad (3.39)$$

The operator product expansion encodes the statistics of rare fluctuations around the path of minimal energy [81, 76] as shown in figure 7. Notice that the *leading* singular term is

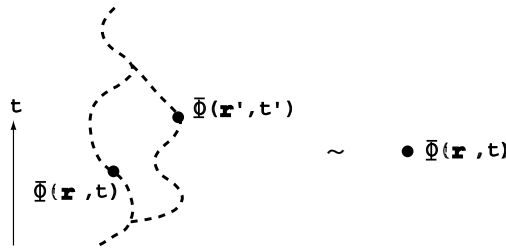


Figure 7. The operator product expansion of contact fields for a string in a disordered medium. The short-distance asymptotics of the pair of fields $\Phi(t)$ and $\Phi(t')$ is given by the single field $\Phi(t)$ multiplied by a singular prefactor. The dashed lines indicate the string configurations generating the singularity $|t - t'|^{-x-\omega}$.

proportional to the irrelevant variable β^{-1} and hence governed by a correction-to-scaling exponent. This is why the temperature is called a dangerous irrelevant variable.

As before, the operator product expansion (3.37) determines the leading ultraviolet singularities of the integrals in (3.32), which appear as poles in $y \equiv 1 - x - \omega$. The defect contribution to the Casimir amplitude can again be written in terms of a dimensionless coupling constant:

$$\Delta \bar{C}(g, R) = R^{x/\zeta} \overline{\langle \Phi \rangle} \left(u - \frac{C}{y} u^2 \right) + O(y^0 u^2, u^3) \tag{3.40}$$

with

$$u \equiv g R^{y/\zeta}. \tag{3.41}$$

Indeed, equation (3.40) remains finite in the limit $\beta^{-1} \rightarrow 0$ for fixed R and g . The pole can be absorbed into the ‘minimally subtracted’ coupling constant $u_M = \mathcal{Z}_M u$ (which should not be confused with the coupling (2.17) defined in perturbation theory about the Gaussian fixed point). With

$$\mathcal{Z}_M(u_M) = 1 - \frac{C}{y} u_M + O(u_M^2) \tag{3.42}$$

the flow equation $\dot{u}_M \equiv \zeta R \partial_R u_M$ reads

$$\dot{u}_M = y u_M - C u_M^2 + O(u_M^3). \tag{3.43}$$

We conclude that an attractive linear defect is less effective in localizing a directed string in a random system than in a pure system, in agreement with some previous approximate renormalization group studies [73, 74, 76]. A weak defect is a relevant perturbation of the zero-temperature fixed point $u_M = 0$ only for dimension $d < 1$. It localizes the string with

$$\xi \sim (-g)^{-\zeta/y} \quad (g < 0). \tag{3.44}$$

For the borderline dimension $d = 1$, the theory is again asymptotically free, with

$$\xi \sim \exp(-C\zeta/g) \quad (g < 0). \tag{3.45}$$

For $d > 1$, a finite defect strength $|g| > |g_c|$ is necessary to localize the string:

$$\xi \sim (g_c - g)^{-\zeta/y^*} \quad (g < g_c) \tag{3.46}$$

where

$$y^* \equiv \lim_{u_M \rightarrow u_M^*} \frac{\dot{u}_M}{u_M^* - u_M} = -y + O(y^2)$$

is the eigenvalue of the flow equation at the non-trivial fixed point. The disorder-averaged string density given by equation (2.28) has the short-distance singularity $\overline{P}(r) \sim r^\theta$ with $\theta = 2y/\zeta + O(y^2) < 0$.

A weak repulsive defect is an irrelevant perturbation of the strong-coupling fixed point for $d \geq 1$. In particular, it does not generate a ‘fermionic’ zero of the string density $P(r)$ in the limit $R \rightarrow \infty$. This prediction of renormalized perturbation theory is consistent with the scaling at a strong repulsive defect or *barrier*, which can be obtained exactly for $d = 1$ [82]. An impenetrable barrier ($g \rightarrow \infty$) is equivalent to a system boundary, leading to a long-ranged depletion $\overline{P}(r) \sim r$ of the string density (see section 3.4). A hardly penetrable barrier has rare crossings that happen whenever the difference between the random energies on the left-hand and right-hand sides of the barrier in a given longitudinal interval Δt exceeds the barrier penalty. Since the string configurations on one side consist of essentially uncorrelated pieces of length $\sim R^{3/2}$, this difference scales as

$$\overline{\Delta F}(\Delta t, R) = (\Delta t)^{1/3} \mathcal{F}_d(\Delta t R^{-3/2}) \sim (\Delta t)^{1/2} R^{-1/4} \tag{3.47}$$

for $\Delta t \gg R^{3/2}$. Hence the path remains on one side of the barrier for a typical longitudinal distance Δt given by $(\Delta t)^{1/2} R^{-1/4} \sim g$. This determines the expectation value of the contact field:

$$\overline{\langle \Phi \rangle} \sim \frac{1}{\Delta t} \sim g^{-2} R^{-1/2}. \tag{3.48}$$

We conclude that the penetrability g^{-2} conjugate to Φ is a relevant perturbation with eigenvalue $y = 1/3$ at the barrier fixed point $g^{-2} = 0$. It induces a crossover to the delocalization fixed point $g = 0$: the barrier becomes irrelevant on large scales.

3.4. A string and a wall

As mentioned above, a half-space Gaussian string $(r_1 > 0, r_2, \dots, r_d)(t)$ in contact interaction with a system boundary at $r_1 = 0$ is equivalent to the string $r_1(t)$ in full space coupled to a defect at $r_1 = 0$. In a random background, this is no longer the case. The disorder potential couples the string coordinates r_1, \dots, r_d , and the boundary has a non-local influence on the string by cutting off all disorder configurations in the half-space $r_1 < 0$. Alternatively, the half-space system can be understood as an unrestricted system with a defect plane at $r_1 = 0$ and ‘mirror’ constraints $\eta(r_1, \dots, r_d, t) = \eta(-r_1, \dots, r_d, t)$ on the random potential [83].

We restrict ourselves here to the case where $d = 1$, where a half-space string with the action (3.29) can be treated exactly by Bethe *ansatz* methods [37] or by mapping onto a lattice gas [84]. One finds a (de-)localization transition with the localization length singularity

$$\xi \sim (g_c - g)^{-2} \quad (g < g_c). \tag{3.49}$$

At the transition, the disorder-averaged string density (2.28) has the singularity (see p 317 of [40])

$$\overline{P}(r) \sim r^{-1/2} R^{-1/2} \quad \text{for } \tilde{r} \ll r \ll R. \tag{3.50}$$

Hence, the boundary contact field $\Phi_b(t) \equiv \delta(r(t))$ has the expectation value

$$\overline{\langle \Phi_b(t) \rangle} \sim R^{-x_b/\zeta} \tag{3.51}$$

with $x_b = 1/3$. As in section 3.3, we then obtain the operator product expansion

$$\Phi_b(t)\Phi_b(t') = C_b \beta^{-1} |t - t'|^{-x_b - \omega} \Phi_b(t) + \dots \tag{3.52}$$

with $C_b > 0$. Hence, the wall changes the statistics of rare fluctuations. This operator product expansion leads again to a beta function of the form (3.43) with $y_b = 1 - x_b - \omega$.

In $d = 1$, the interaction with the wall is a truly relevant perturbation with eigenvalue $y_b = 1/3$ at the (de-)localization point. This leads to a singularity (3.44) of the localization length, which agrees with (3.49) and with the result of [43] obtained from a variational scaling argument for the bound-state free energy. For $g > g_c$, there is a crossover to the fixed point $u_M^* = y_b/C_b + O(y_b^2)$ with exponents $x^* = 1 - \omega + y_b + O(y_b^2)$ and $\theta = x^*/\zeta - d > 0$ describing a long-ranged depletion of the string density $\overline{P}(r)$. This is again in agreement with exact results [84] and numerical transfer matrix studies [85] but the one-loop calculation underestimates the true value $\theta = 1$.

3.5. Strings with mutual interactions

The effective action

$$S[\mathbf{r}_1, \mathbf{r}_2, \eta] = \int dt \left(\frac{1}{2} \sum_{i=1}^2 \left(\frac{d\mathbf{r}_i}{dt} \right)^2 + \sum_{i=1}^2 \eta(\mathbf{r}_i(t), t) + g\Psi(t) \right) \quad (3.53)$$

with the contact field $\Psi(t) \equiv \delta(\mathbf{r}_1(t) - \mathbf{r}_2(t))$ describes a pair of directed strings that ‘live’ in the same random medium and are coupled by short-ranged mutual forces [77–80, 46]. In the case of flux lines, for example, this interaction is repulsive. Due to the random potential, the centre-of-mass displacement of the strings does not decouple from their relative displacement. The two-string system is therefore not equivalent to a single string and a linear defect.

The effects of pair interactions turn out to be much stronger than in a pure system. Qualitatively, this is easy to understand. At zero temperature, two non-interacting strings in the same random potential share a common minimal path $\mathbf{r}_0(t)$. At small but finite temperatures, it turns out that the strings still follow a ‘tube’ of width \tilde{r} around $\mathbf{r}_0(t)$ with finite probability. Hence, their overlap probability $\overline{\langle \Psi(t) \rangle}$ remains finite in the limit $R \rightarrow \infty$, in contrast to that of non-interacting thermal strings, $\langle \Psi(t) \rangle \sim R^{-d\zeta_0}$. This explains the great sensitivity of the system to repulsive forces. However, the strings make large individual excursions from the tube. The disorder-averaged pair density (2.28) (with $\mathbf{r} = \mathbf{r}_1 - \mathbf{r}_2$) has the form [81, 46]

$$\overline{P}(r) \sim \beta^{-1} r^{-d-\omega/\zeta} \quad \text{for } r \gtrsim \tilde{r} \text{ and } R \rightarrow \infty \quad (3.54)$$

dictated by the operator product expansion (3.39). A strong repulsion ($g \rightarrow \infty$) forces one of the strings onto the lowest excited path $\mathbf{r}_1(t)$ that has no overlap with $\mathbf{r}_0(t)$ (with fluctuations of the form (3.54) around $\mathbf{r}_1(t)$ at finite temperatures). The paths $\mathbf{r}_1(t)$ and $\mathbf{r}_0(t)$ have an average distance of order R , and the pair density should have a long-ranged depletion $\overline{P}(r) \sim r^\theta$ with $\theta > 0$ for $g \rightarrow \infty$, just like that of free fermions for $d = 1$. At the strong-coupling fixed point of non-interacting strings, the pair field $\Psi(t)$ is therefore a relevant perturbation inducing the crossover to the ‘fermionic’ behaviour for $g \rightarrow \infty$.

This argument can be made quantitative [46]. We start from the expansion

$$\Delta\overline{C}(g, R) = -\beta^{-1} R^{(1-\omega)/\zeta} \sum_{N=1}^{\infty} \frac{(-\beta g)^N}{N!} \int dt_2 \cdots dt_N \overline{\langle \Psi(0)\Psi(t_2)\cdots\Psi(t_N) \rangle^c} \quad (3.55)$$

of the Casimir amplitude (3.31) about the strong-coupling fixed point of non-interacting strings ($g = 0$). Since the overlap probability of the two strings

$$\overline{\langle \Psi(t) \rangle} \sim R^{-x/\zeta} \quad (3.56)$$

remains finite as $R \rightarrow \infty$, the local field $\Psi(t)$ has dimension $x = 0$. The connected correlation functions of $\Psi(t)$ vanish at zero temperature, as do those of the contact field $\Phi(t)$ of section 3.3. One obtains an operator product expansion of the form (3.37):

$$\Psi(t)\Psi(t') = C_2\beta^{-1}|t - t'|^{-\omega}\Psi(t) + \dots \tag{3.57}$$

with $C_2 > 0$. Its leading term is again a correction to scaling proportional to the dangerous irrelevant variable β^{-1} . Renormalization of the perturbation series (3.55) then leads to the flow equation (3.43) with $y = 1 - \omega$.

It follows that an attractive pair interaction always localizes the strings. The pair density $\overline{P}(r, \xi)$ of the localized state has the form

$$\overline{P}(r, \xi) \sim \beta^{-1}r^{-d-\omega/\zeta}\mathcal{P}(r/\xi) \quad \text{for } r \gtrsim \tilde{r}. \tag{3.58}$$

The scaling function \mathcal{P} has a finite limit at short distances and decays exponentially on scales $r \gtrsim \xi$. The localization length ξ has the singularity

$$\xi \sim (-g)^{-\zeta/y} = (-g)^{(1+\omega)/2(1-\omega)} \quad (g < 0). \tag{3.59}$$

The transverse scale $\xi^{(m)}$ defined by the m th moment of the pair density

$$\xi^{(m)} \equiv \left(\int dr r^m \overline{P}(r, \xi) \right)^{1/m} \quad (m = 1, 2, \dots) \tag{3.60}$$

scales as

$$\xi^{(m)} \sim \beta^{-1/m}(-g)^{-(\zeta-\omega/m)/y} \quad (g < 0). \tag{3.61}$$

Recall that at an ordinary fixed point, all the scales $\xi^{(m)}$ have the same exponent as the correlation length ξ . The dangerous irrelevant variable β^{-1} breaks this universality and induces the *multiscaling* (3.61). A similar phenomenon occurs for directed strings with thermal fluctuations in dimensions $d > 4$ [58].

Repulsive forces lead to an asymptotic scaling $\overline{P}(r) \sim r^\theta$ with $\theta = x^*/\zeta - d$ given in terms of the dimension $x^* = 2(1 - \omega) + O((1 - \omega)^2)$ of the pair field at the non-trivial fixed point. A numerical transfer-matrix study of a pair of strongly repulsive strings ($g \rightarrow \infty$) confirms the long-ranged depletion of the pair density [85]. The exponent $\theta \approx 2$ is underestimated by the one-loop calculation.

The above considerations are valid only as long as d is below the upper critical dimension $d_>$ of a single string. This can be seen as follows. It is possible to show that the ground-state path $\mathbf{r}_0(t)$ is unique (up to microscopic degeneracies of the order of the lattice spacing) in almost all realizations of the disorder [38, 81]. This uniqueness is also manifest in the pair density (3.54): for any fixed $r_0 > 0$, the probability of finding the strings at a relative distance $r > r_0$ remains finite for $R \rightarrow \infty$, and that limit value tends to zero for $\beta^{-1} \rightarrow 0$ [46]:

$$\int_{r>r_0} dr \overline{P}(r) \sim \beta^{-1}r_0^{-\omega/\zeta}. \tag{3.62}$$

However, for $d \rightarrow d_>$ (i.e., $\omega \rightarrow 0$), the pair distribution (3.54) shows a singular broadening: for $R \rightarrow \infty$ and fixed β^{-1} , the probability (3.62) approaches one. Consequently, the overlap probability (3.56) goes to zero, $\langle \Psi(t) \rangle \sim \omega$. This suggests that the statistics of string configurations becomes more complicated for $d \geq d_>$. The strings no longer cluster in the vicinity of the minimal path as expressed by (3.62), but exploit multiple near-minimal paths at any finite temperature. Their overlap $\langle \Psi(t) \rangle$ is expected to vanish for $R \rightarrow \infty$.

3.6. The upper critical dimension of a single string

The theory of strings with pair interactions discussed in section 3.5 has an important implication for the single-string system [47]: the upper critical dimension of a single string is less than or equal to four. As $d_>$ is approached from below, the exponents ζ and ω tend to the Gaussian values $\zeta = 1/2$ and $\omega = 0$ continuously. Hence, the upper critical dimension could serve as the starting point for a controlled expansion. The name ‘upper critical dimension’ is, however, quite misleading, since $d_>$ does not mark the borderline with simple mean-field behaviour as in the standard theory of critical phenomena. On the contrary, the state of the system in high dimensions may be even more complicated, having presumed glassy characteristics [86, 31].

The existence of an upper critical dimension has been controversial. Numerical work seems to indicate that a strong-coupling phase with non-trivial exponents $z < 2$, $\chi > 0$ persists for dimensions $d = 4$ and higher [26–28]. However, the results for $d > 3$ are not very reliable since the available system sizes are limited and corrections to scaling are not taken into account [48].

Various theoretical arguments favour the existence of a finite upper critical dimension $d_>$ at or slightly below four. Most of these approaches rest on approximation schemes (such as functional renormalization [29, 30] or mode-coupling theory [31]) whose status is not very well understood. The same is true for a recent approximate real-space renormalization [87] challenging these results.

The argument given here [47] is of a different nature; it is not tied to any of these approximation schemes. An important ingredient is (3.61), a set of *exact* relations in the strong-coupling regime. These relations describe the bound state (3.58) of attractively coupled strings in terms of the only independent single-string exponent $\omega = 2\zeta - 1$. We focus on the temperature dependence of the scales $\xi^{(m)}$. For fixed g , $\xi^{(m)}$ is monotonically increasing with temperature according to (3.61). This is not surprising since it is temperature-driven fluctuations of the strings around the path $\mathbf{r}_0(t)$ that generate the pair distribution (3.58). At the roughening transition (i.e., for $\beta^{-1} = \beta_c^{-1}$), the singularity of $\xi^{(m)}$ changes:

$$\xi^{(m)} \sim \xi \sim (-g)^{-\zeta^*/y^*} \quad \text{with } y^* = (d - 2)/2 \quad (3.63)$$

as discussed in section 3.1. With the natural assumption that $\xi^{(m)}$ remains a monotonic function of β^{-1} for all $\beta^{-1} \leq \beta_c^{-1}$ and fixed g , one then obtains the inequalities $y/(\zeta - \omega/m) \geq y^*/\zeta^*$. These imply an upper bound on the free-energy exponent:

$$\omega \leq \frac{4 - d}{d}. \quad (3.64)$$

The result $d_> \leq 4$ then follows immediately.

It is tempting to speculate about the nature of the strong-coupling regime in high dimensions. Below $d_>$, the pair distribution of non-interacting strings at fixed temperature has the finite limit (3.54) for $R \rightarrow \infty$, and this limit distribution collapses to $\delta(\mathbf{r}_1 - \mathbf{r}_2)$ for $\beta^{-1} \rightarrow 0$. For $d \geq d_>$, the pair distribution is expected to depend on both β^{-1} and R in an essential way. Its asymptotic behaviour will then depend on the order in which the zero-temperature limit and the thermodynamic limit $R \rightarrow \infty$ are taken. Similar properties are familiar from glassy systems.

3.7. Discussion

Interacting strings in a random background turn out to have a rich scaling behaviour. In one transverse dimension alone, there are no less than six universality classes characterized

by of the exponent θ of the disorder-averaged string density and the renormalization group eigenvalue y of the contact coupling. These universality classes describe

- (i) the (de-)localization transition of a string at a linear defect ($\theta = 0, y = 0$),
- (ii) the (de-)localization transition of a string at an attractive wall ($\theta = -1/2, y = 1/3$),
- (iii) the (de-)localization transition of a pair of strings with contact attraction ($\theta = -3/2, y = 2/3$),
- (iv) the scaling of a string at a barrier ($\theta = 1, y = 1/3$),
- (v) the scaling of a string at a repulsive wall ($\theta = 1, y = -2/3$),
- (vi) the scaling of a pair of strings with contact repulsion ($\theta = 2, y = -4/3$).

Clearly, the list could be continued by including higher dimensions, long-ranged interactions or disorder correlations etc. Recall from section 2 that without quenched disorder, the six cases are described by just two universality classes, namely Gaussian strings ($\theta = 0, y = 1/2$) and free fermions ($\theta = 2, y = -1/2$).

This scenario is consistent with an operator product expansion (3.37) of the contact field, which is the basis for perturbation theory about the strong-coupling fixed point. The existence of an operator product expansion is of conceptual importance since the correlations in the strong-coupling regime are generated by global minimization of the free energy and not by a local action. The operator product expansion explicitly contains the temperature β^{-1} as dangerous irrelevant variable. This variable, which is proportional to the surface tension ν of the associated KPZ surface, will prove dangerous in the growth problem as well: it generates the dynamical anomaly discussed in the next section.

4. Directed growth

All of the methods and results on directed polymers in a random medium discussed in the previous section have their correspondences in KPZ surface growth via the Hopf–Cole transformation (1.7). In particular, the KPZ equation has an upper critical dimension less than or equal to four (see section 3.6).

To discuss dynamical renormalization, we rewrite equation (1.1) as a path integral for the height field $h(\mathbf{r}, t)$ and the response field $\tilde{h}(\mathbf{r}, t)$. It proves necessary to distinguish carefully between renormalized fields and couplings defined in a non-perturbative way, and perturbatively renormalized quantities defined, for example, by minimal subtraction. The perturbative renormalization of the dynamic path integral is seen to be equivalent to the replica perturbation theory of section 3: it captures the roughening transition but does not produce a fixed point corresponding to the strong-coupling regime [18]. This failure of perturbation theory is explained by the fact that the non-perturbatively renormalized coupling constant u and the corresponding height field h (defined by conditions on correlation functions at a renormalization point) have a singular dependence on their perturbatively subtracted counterparts u_P and h_P .

The strong-coupling regime thus calls for non-perturbative methods. In the second part of this section, we analyse constraints on the effective growth dynamics imposed by the consistency of correlation functions. The consistency relations again take the form of an operator product expansion. The response field \tilde{h} is found to obey an operator product expansion similar to those of the previous section [45]. The resulting structure of the response functions is tied to KPZ growth with additional deterministic driving forces. In particular, a surface with a local variation $-(g/\lambda)\delta(\mathbf{r})$ in the deposition rate corresponds to a directed string interacting with a linear defect (see section 3.3). It turns out that (for $\lambda > 0$) a sufficiently enhanced deposition ($g/\lambda < g_c/\lambda$) induces an increased growth rate even in

the thermodynamic limit $R \rightarrow \infty$, while for $g/\lambda > g_c/\lambda$ the growth rate is asymptotically independent of g [88, 73]. These two regimes are separated by a non-equilibrium phase transition, the analogue of the string (de-)localization transition.

Finally, we turn to the correlations of the height field [49]. These are assumed to obey an operator product expansion as well. Consistently with the available numerical data, we further assume that these correlations do not show multiscaling, unlike the correlations in a turbulent fluid. This property constrains severely the possible form of the operator product expansion. A discrete set of values of the roughness exponent emerges:

$$\chi = \frac{2}{k_0 + 2} \quad \text{with } k_0 = 1, 2, \dots \tag{4.1}$$

Only for these values does the KPZ equation admit solutions with a *dynamical anomaly* in the strong-coupling regime. It is argued on phenomenological grounds that the scaling of growing surfaces should be governed by such solutions with an odd value of k_0 . Hence the exact values of the growth exponents for two- and three-dimensional surfaces are derived.

4.1. Field theory of the Kardar–Parisi–Zhang model

The path integral formulation [89] of the stochastic evolution (1.1), (1.2) is obtained in a straightforward way. We rewrite the Gaussian distribution of the driving force $\eta(\mathbf{r}, t)$:

$$\int \mathcal{D}\eta \exp\left(-\int d\mathbf{r} dt \frac{1}{2\sigma^2} \eta^2\right) = \int \mathcal{D}\eta \mathcal{D}\tilde{h} \exp\left(-\int d\mathbf{r} dt \left(-\frac{\sigma^2}{2} \tilde{h}^2 + \tilde{h}\eta\right)\right) \tag{4.2}$$

introducing the purely imaginary ‘ghost’ field $\tilde{h}(\mathbf{r}, t)$. Eliminating η by using the equation of motion, we obtain the (Itô-discretized) path integral

$$Z = \int \mathcal{D}h \mathcal{D}\tilde{h} \exp\left[-\int d\mathbf{r} dt \left(-\frac{\sigma^2}{2} \tilde{h}^2 + \tilde{h}\left(\frac{\partial}{\partial t} h - \frac{v}{2} \nabla^2 h - \frac{\lambda}{2} (\nabla h)^2\right)\right)\right] \tag{4.3}$$

the generating functional of the dynamical correlations. Ghost-field insertions produce the response functions

$$\left\langle \prod_{j=1}^{\tilde{N}} \tilde{h}(\mathbf{r}_j, t_j) \prod_{j=\tilde{N}+1}^{\tilde{N}+N} h(\mathbf{r}_j, t_j) \right\rangle = \prod_{j=1}^{\tilde{N}} \frac{\delta}{\delta \rho(\mathbf{r}_j, t_j)} \left\langle \prod_{j=\tilde{N}+1}^{\tilde{N}+N} h(\mathbf{r}_j, t_j) \right\rangle \tag{4.4}$$

where $\rho(\mathbf{r}, t)$ is an additional source field in the equation of motion:

$$\partial_t h = v \nabla^2 h + \frac{\lambda}{2} (\nabla h)^2 + \eta + \rho. \tag{4.5}$$

There is a third way to express the KPZ dynamics. Writing the equal-time height correlations in the form

$$\langle h(\mathbf{r}_1, t) \cdots h(\mathbf{r}_n, t) \rangle \equiv \langle h(\mathbf{r}_1) \cdots h(\mathbf{r}_n) \rangle_t = \int \mathcal{D}h h(\mathbf{r}_1) \cdots h(\mathbf{r}_n) P_t \tag{4.6}$$

the time dependence has been shifted from the field variables $h(\mathbf{r}, t)$ to the configuration weight $P_t[h]$. The latter obeys the functional Fokker–Planck equation

$$\partial_t P_t = \int d\mathbf{r} \left(\sigma^2 \frac{\delta^2}{\delta h(\mathbf{r})^2} - \frac{\delta}{\delta h(\mathbf{r})} J(\mathbf{r}) \right) P_t \tag{4.7}$$

where

$$J(\mathbf{r}) \equiv v \nabla^2 h(\mathbf{r}) + \frac{\lambda}{2} (\nabla h)^2(\mathbf{r}) \tag{4.8}$$

is the deterministic part of the current.

In the linear theory, the fields $h(\mathbf{r}, t)$ and $\tilde{h}(\mathbf{r}, t)$ have canonical dimensions $-\chi_0 = (d - 2)/2$ and $\chi_0 + d = (d + 2)/2$, respectively, and the dynamical exponent is $z_0 = 2$ (the basic scale is now that of \mathbf{r}).

A crucial role in the following will be played by the infrared divergencies of the height correlations [49]. Their physical meaning can be seen already in the linear theory, which has the response propagator

$$\langle \tilde{h}(\mathbf{r}_1, t_1) h(\mathbf{r}_2, t_2) \rangle = \frac{\theta(t_2 - t_1)}{(2\pi\nu(t_2 - t_1))^{d/2}} \exp\left(-\frac{(\mathbf{r}_1 - \mathbf{r}_2)^2}{2\nu(t_2 - t_1)}\right) \quad (4.9)$$

($\theta(t)$ denoting the step function) and the height–height correlation function

$$\langle h(\mathbf{r}_1, t_1) h(\mathbf{r}_2, t_2) \rangle = \sigma^2 \int d\mathbf{r} dt \langle \tilde{h}(\mathbf{r}, t) h(\mathbf{r}_1, t_1) \rangle \langle \tilde{h}(\mathbf{r}, t) h(\mathbf{r}_2, t_2) \rangle. \quad (4.10)$$

However, the last expression is divergent in infinite space for $d < 2$ (i.e., $\chi_0 > 0$). Therefore, it depends strongly on the initial or boundary conditions. For stationary growth in a system of size R , the dominant part in the limit $R \rightarrow \infty$ is

$$\langle h(\mathbf{r}_1, t_1) h(\mathbf{r}_2, t_2) \rangle_R \sim \langle h^2 \rangle_R \sim R^{2\chi} \quad (4.11)$$

where $\langle h^2 \rangle \equiv \langle h^2(\mathbf{r}_1, t_1) \rangle = \langle h^2(\mathbf{r}_2, t_2) \rangle$ with periodic boundary conditions. The amplitude (4.11) measures the *global* roughness of the surface, i.e., the size of its mountains and valleys. The regularized height correlation, however, can be written in terms of height differences measuring the *local* roughness:

$$\langle h(\mathbf{r}_1, t_1) h(\mathbf{r}_2, t_2) \rangle_R - \langle h^2 \rangle_R = -\frac{1}{2} \langle (h(\mathbf{r}_1, t_1) - h(\mathbf{r}_2, t_2))^2 \rangle_R. \quad (4.12)$$

The finite limit for $R \rightarrow \infty$

$$\langle (h(\mathbf{r}_1, t_1) - h(\mathbf{r}_2, t_2))^2 \rangle = |\mathbf{r}_1 - \mathbf{r}_2|^{2\chi_0} \mathcal{G}_0\left(\frac{\nu|t_1 - t_2|}{(\mathbf{r}_1 - \mathbf{r}_2)^2}\right) \quad (4.13)$$

shows (affine) scale invariance. In the interacting theory, the infrared regularization is more complicated since the higher connected height correlations also develop R -dependent singularities. But the local statistics of the surface, measured by height differences, is still expected to remain finite for $R \rightarrow \infty$, i.e., to decouple from the divergent amplitudes.

The interacting theory has an ultraviolet singularity as well. Taking the expectation value of the equation of motion, we obtain the growth rate, which has the form

$$\langle \partial_t h \rangle_R = \frac{\lambda}{2} \langle (\nabla h)^2 \rangle_R \sim a^{2\chi-2} + \mathcal{O}(R^{2\chi-2}) \quad (4.14)$$

for stationary growth. The dependence on the short-distance cut-off a can be removed by the subtraction

$$\langle (\nabla h)^2 \rangle \rightarrow \langle (\nabla h)^2 \rangle - \langle (\nabla h)^2 \rangle_\infty \quad (4.15)$$

which affects the one-point function $\langle h(\mathbf{r}, t) \rangle$ but leaves the higher connected correlation functions invariant. This normal ordering of the interaction field will always be implied in the following. The nature of the cut-off-dependent term in (4.14) is clear from the mapping onto directed strings. Via equation (1.7), the subtracted growth rate is directly related to the Casimir term (3.31):

$$-\lambda \langle \partial_t h \rangle_R = \bar{f}(R) \quad (4.16)$$

while the a -dependent term contributes to the non-universal part of the free energy.

4.2. Dynamical perturbation theory

Perturbation theory for the KPZ dynamics can be set up in different ways.

(a) The standard formalism is a diagrammatic expansion of the path integral (4.3) with interaction vertex $\tilde{h}(\nabla h)^2$ about the Gaussian limit $\lambda = 0$. The propagators of the Gaussian theory are the response function $\langle \tilde{h}(\mathbf{r}_1, t_1) h(\mathbf{r}_2, t_2) \rangle$ and the correlation function $\langle h(\mathbf{r}_1, t_1) h(\mathbf{r}_2, t_2) \rangle$; see equations (4.9) and (4.10). Renormalization is usually based on the expansion of the Fourier-transformed two-point functions $\langle \tilde{h}(-\mathbf{k}, -\omega) h(\mathbf{k}, \omega) \rangle$ and $\langle h(-\mathbf{k}, -\omega) h(\mathbf{k}, \omega) \rangle$. This has been carried out to first [15, 16] and second order [90, 17]; see also the criticism in [81, 91]. In the appendix, we discuss instead the expansion for the real-space response function $\langle \tilde{h}(\mathbf{r}_1, t_1) h(\mathbf{r}_2, t_2) \rangle$ and the universal part of the growth rate $\langle \partial_t h \rangle_R$ in order to exhibit the analogy with the replica perturbation theory of section 3.1. Beyond leading order, however, calculations become cumbersome in this formalism.

(b) By performing the Hopf–Cole transformation (1.7) and the corresponding transformation of the response field [45]

$$h = \frac{2\nu}{\lambda} \log \phi \quad \tilde{h} = \frac{\lambda}{2\nu} \bar{\phi} \phi \tag{4.17}$$

the path integral (4.3) can be brought to the form [92]

$$Z = \int \mathcal{D}\phi \mathcal{D}\bar{\phi} \exp \left[-\frac{1}{2\nu} \int d\mathbf{r} dt \left(\bar{\phi}(\partial_t - \nu \nabla^2)\phi - \frac{\sigma^2 \lambda^2}{2\nu} \bar{\phi}^2 \phi^2 \right) \right] \tag{4.18}$$

which equals the replica action (3.9) introduced previously in reference [18] (with $\beta = 1/2\nu$ and $\lambda = 1$). We emphasize, however, that (4.18) is not a faithful representation of the growth dynamics unless it is defined with boundary conditions enforcing the limit $p \rightarrow 0$; see the discussion in the appendix. The theory is now Gaussian for finite λ but $\sigma^2 = 0$. The propagator $\langle \bar{\phi}(\mathbf{r}_1, t_1) \phi(\mathbf{r}_2, t_2) \rangle$ is again given by (4.9); the interaction vertex $\bar{\phi}^2 \phi^2$ arises from the noise term \tilde{h}^2 . The resulting diagrammatic expansion is identical to the replica perturbation theory of section 3 and can hence be renormalized exactly to all orders, as shown in the appendix.

In both cases, the expansion parameter is again the dimensionless coupling constant $u_0 = g_0 R^{2\nu_0}$ with

$$g_0 = \frac{\sigma_0^2 \lambda_0^2}{(2\nu_0)^3} \tag{4.19}$$

where the fields and couplings of the bare theory are labelled by the subscript 0. The poles in y_0 can be absorbed into loopwise-subtracted fields h_P, \tilde{h}_P and the coupling constant $u_P = \mathcal{Z}_P u_0$ given by (A.13). There is no renormalization of $t_0 = t_P$, which would be required in the strong-coupling regime according to (3.27).

The flow equation is again (2.24) with the fixed point $u_P^* = y_0/C_0$ representing the roughening transition for $2 < d < 4$. At the transition, the Casimir amplitude of the growth rate takes a finite value regular in y_0 :

$$R^2 \frac{\lambda_c}{(2\nu)^2} \langle \partial_{t_P} h_P \rangle_R = \frac{1}{4} \frac{y_0}{C_0} + \mathcal{O}(y_0^2) \tag{4.20}$$

which is directly related to the Casimir amplitude (3.14) of a string in a random medium. The scaling exponents at the transition

$$\chi^* = 0 \quad z^* = 2 \tag{4.21}$$

are independent of d , in agreement with the finite-order calculations of [15–17]. These exponents have been predicted previously by a scaling argument [93].

4.3. Renormalization beyond perturbation theory

Of course, renormalization is not tied to a loopwise expansion and can be defined in a non-perturbative way [18]. The correlation functions show crossover scaling from the linear to the strong-coupling regime ($d \leq 2$) and from the critical to the strong-coupling regime ($d > 2$). The crossover has the characteristic scales \tilde{r} and \tilde{t} given by (3.22) with $\beta^{-1} = 2\nu$.

For $d \leq 2$, the response and correlation functions have the scaling form

$$\left\langle \prod_{j=1}^{\tilde{N}} \tilde{h}_0(\mathbf{r}_j, t_{0j}) \prod_{j=\tilde{N}+1}^{\tilde{N}+N} h_0(\mathbf{r}_j, t_{0j}) \right\rangle = R^{-N\chi_0 + \tilde{N}(\chi_0 + d)} \mathcal{G}_{N\tilde{N}} \left(\frac{\mathbf{r}_j - \mathbf{r}_k}{R}, \frac{t_{0j} - t_{0k}}{R^{z_0}}, u_0 \right). \quad (4.22)$$

Equation (4.22) can be written as the bare Callan–Symanzik equation

$$\left(R \frac{\partial}{\partial R} \Big|_{\lambda_0} + \sum_j \mathbf{r}_j \frac{\partial}{\partial \mathbf{r}_j} + z_0 \sum_j t_{0j} \frac{\partial}{\partial t_{0j}} + \dot{u}_0 \frac{\partial}{\partial u_0} - N\chi_0 + \tilde{N}(\chi_0 + d) \right) \times \left\langle \prod_{j=1}^{\tilde{N}} \tilde{h}_0(\mathbf{r}_j, t_{0j}) \prod_{j=\tilde{N}+1}^{\tilde{N}+N} h_0(\mathbf{r}_j, t_{0j}) \right\rangle = 0 \quad (4.23)$$

with

$$\dot{u}_0 \equiv R \partial_R u_0 = 2y_0 u_0. \quad (4.24)$$

For the infrared-regularized correlators, the explicit dependence on R vanishes in the thermodynamic limit.

In the strong-coupling regime, these correlation functions develop anomalous scaling and hence a singular dependence on the bare coupling constant u_0 . Renormalization consists in absorbing these singularities into new variables:

$$\begin{aligned} h &= \mathcal{Z}_h h_0 \\ \tilde{h} &= \mathcal{Z}_h^{-1} \tilde{h}_0 \\ t &= \mathcal{Z}_t t_0 \\ u &= \mathcal{Z} u_0 = \mathcal{Z}_h^{-2} \mathcal{Z}_t^{-2} u_0. \end{aligned} \quad (4.25)$$

The \mathcal{Z} -factors can all be written as functions of u .

Under this change of variables, equation (4.23) transforms into the renormalized Callan–Symanzik equation

$$\left(R \frac{\partial}{\partial R} \Big|_{\lambda_0} + \sum_j \mathbf{r}_j \frac{\partial}{\partial \mathbf{r}_j} + z(u) \sum_j t_j \frac{\partial}{\partial t_j} + \dot{u} \frac{\partial}{\partial u} - N\chi(u) + \tilde{N}(\chi(u) + d) \right) \times \left\langle \prod_{j=1}^{\tilde{N}} \tilde{h}(\mathbf{r}_j, t_j) \prod_{j=\tilde{N}+1}^{\tilde{N}+N} h(\mathbf{r}_j, t_j) \right\rangle = 0 \quad (4.26)$$

with

$$\dot{u} \equiv R \partial_R u = \frac{2y_0 u}{1 - u (d/du) \log \mathcal{Z}} \quad (4.27)$$

$$z(u) = z_0 - \dot{u} \frac{d}{du} \log \mathcal{Z}_t \quad (4.28)$$

$$\chi(u) = \chi_0 - \dot{u} \frac{d}{du} \log \mathcal{Z}_h. \quad (4.29)$$

Notice that only two of the \mathcal{Z} -factors are independent. The ghost-field renormalization is tied to that of h since the response function $\langle \tilde{h}(\mathbf{r}_1, t_1)h(\mathbf{r}_2, t_2) \rangle$ always has dimension d by definition. Furthermore, Galilei invariance implies the relation $\mathcal{Z} = \mathcal{Z}_h^{-2}\mathcal{Z}_t^{-2}$ obtained by inserting the exponent relation $\chi + z = 2$ into (4.27), (4.28), and (4.29). A different but equivalent Callan–Symanzik equation is derived in [17].

The renormalized variables (4.25) can be defined in a non-perturbative way by means of two independent normalization conditions. These are imposed, e.g., on the stationary two-point functions in an infinite system:

$$R^{2\chi_0} \langle (h(0, t) - h(R, t))^2 \rangle(u) = R^{2\chi_0} \langle (h_0(0, t_0) - h_0(R, t_0))^2 \rangle(0) \tag{4.30}$$

$$R^d \langle \tilde{h}(\mathbf{r}, t)h(\mathbf{r}, t + R^2) \rangle(u) = R^d \langle \tilde{h}_0(\mathbf{r}, t_0)h_0(\mathbf{r}, t_0 + R^2) \rangle(0). \tag{4.31}$$

R is now an arbitrary normalization scale. An alternative to (4.30) is the normalization condition

$$R^{2-\chi_0} \langle \partial_t h \rangle_R(u) = -\frac{1}{2}u \tag{4.32}$$

on the universal finite-size correction to the stationary growth velocity in a system of size R . Comparing (4.30) and (4.31) with the asymptotic scaling of the bare functions obtained from (4.22)

$$\langle (h_0(\mathbf{r}_1, t_0) - h_0(\mathbf{r}_2, t_0))^2 \rangle \sim \tilde{r}^{-2(\chi-\chi_0)} |\mathbf{r}_1 - \mathbf{r}_2|^{2\chi} \tag{4.33}$$

$$\langle \tilde{h}_0(\mathbf{r}, t_{01})h_0(\mathbf{r}, t_{02}) \rangle \sim \tilde{t}_0^{d/z-d_0/z_0} (t_{02} - t_{01})^{-d/z} \tag{4.34}$$

we infer the asymptotic behaviour of the \mathcal{Z} -factors:

$$\mathcal{Z}_h \sim (\tilde{r}/R)^{\chi-\chi_0} \quad \mathcal{Z}_t \sim (\tilde{r}/R)^{z-z_0}. \tag{4.35}$$

The renormalized height correlation and response functions have a finite continuum limit $\tilde{r} \rightarrow 0$. Of course, this does not imply that all observables are finite in this limit since composite fields may generate additional singularities. However, as discussed in section 4.5, the structure of composite fields of the KPZ theory is expected to be quite simple. All negative-dimensional fields (for example, the monomials $h^k(\mathbf{r})$) have scaling dimensions given by the linear spectrum (4.51). Consequently, the transformations (4.25) do renormalize the correlations of these fields.

The renormalized height field $h(\mathbf{r}, t)$ obeys again an equation of motion of the form (1.1) but the coefficients become singular in the limit $\tilde{r} \rightarrow 0$. By substituting the renormalized variables (4.25) into (1.1), (4.3) or (4.7), we obtain

$$\begin{aligned} v &= \mathcal{Z}_t^{-1}v_0 \simeq v^*(\tilde{r}/R)^\chi \\ \sigma^2 &= \mathcal{Z}_h^2\mathcal{Z}_t^{-1}\sigma_0^2 \simeq \sigma^{*2}(\tilde{r}/R)^{d-2+3\chi} \\ u &= u_0\mathcal{Z}_t^{-2}\mathcal{Z}_h^{-2} \simeq u^* \end{aligned} \tag{4.36}$$

with finite limit values v^* , σ^{*2} , and g^* . Galilei invariance is reflected in the asymptotic scale invariance of the dimensionless coupling, $u \simeq u^*$. This is the non-perturbative strong-coupling fixed point. The other coefficients become irrelevant as $\tilde{r}/R \rightarrow 0$. In particular, we recover the scaling (3.28) of the renormalized temperature $\beta^{-1} = 2v$. It is easy to verify that the strong-coupling asymptotics (4.35) and (4.36) remains unchanged for $d > 2$ although the scaling functions (4.22) now contain singularities marking the roughening transition.

We emphasize again that the existence of this finite continuum limit depends only on the existence of a well-defined scaling regime at large distances. We have not assumed perturbative renormalizability, i.e., that the \mathcal{Z} -factors can be computed as power series in u_0 . It is instructive, however, to compare the renormalized theory with the perturbatively finite

theory of section 4.2. Recall that in a usual ε -expansion, imposing normalization conditions like (4.30), (4.31) is equivalent to requiring finiteness order by order in perturbation theory. The respective coupling constants, u and u_P , are related by a diffeomorphism that remains regular in the limit $\varepsilon \rightarrow 0$ and is defined on a domain of interaction space that contains the fixed points $u_P = u = 0$ and $u^*(u_P^*)$. This equivalence is lost in the crossover to the strong-coupling fixed point. To see this, we integrate the flow equation (2.24) for u_P in two dimensions with the initial condition $u_P(R_0) = u_1$. The solution

$$u_P(R) = \frac{u_1}{1 - u_1 \log(R/R_0)} \tag{4.37}$$

diverges at a finite value $R = R_1 \equiv R_0 \exp(1/u_1)$. It follows immediately that $u_P(R)$ is not a good parametrization of the crossover. The pole of $u_P(R)$ is only a ‘coordinate singularity’ [94] of perturbative subtraction schemes; any renormalized coupling $u(R)$ is expected to remain regular at $R = R_1$. Hence the function $u_P(u)$ has a pole at the value $u(R_1)$ between the fixed points $u = 0$ and u^* . Accordingly, the loopwise-subtracted correlation functions at the normalization point become singular as well: perturbative subtraction fails to maintain a smooth crossover of the large-distance regime.

4.4. Response functions in the strong-coupling regime

The correspondence between directed strings in a random medium and growing surfaces extends to strings with additional interactions. We restrict ourselves here to the case of a string and a linear defect discussed in section 3.3 to infer the properties of the renormalized ghost-field correlations at the strong-coupling fixed point.

The action (3.29) translates into the growth equation

$$\partial_t h = \nu \nabla^2 h + \frac{\lambda}{2} (\nabla h)^2 + \eta - \frac{g}{\lambda} \delta(\mathbf{r}) \tag{4.38}$$

(see references [88, 73]). The extra term describes a spatial inhomogeneity in the average rate of mass deposition onto the surface. The Casimir amplitude (3.30) of the free energy is that of the growth rate:

$$\Delta \bar{C}(g, R) = -\lambda R^{-\chi+z} (\langle \partial_t h \rangle_R(g) - \langle \partial_t h \rangle_R(0)). \tag{4.39}$$

For $g/\lambda < 0$ ($d \leq 1$) and $g/\lambda < g_c/\lambda$ ($d > 1$), translational invariance is strongly broken. The string bound state corresponds to a surface state with a macroscopic stationary mountain

$$H(r) \equiv \langle h(0, t) \rangle - \langle h(\mathbf{r}, t) \rangle \tag{4.40}$$

generating an enhanced growth rate even in the limit $R \rightarrow \infty$.

The inhomogeneity in equation (4.38) contributes a term

$$-(g/\lambda) \int dt \tilde{h}(0, t)$$

to the dynamic action in (4.3). Hence, the perturbation theory (3.32) for the Casimir amplitude (3.30) can be reproduced in the dynamical formalism [45]:

$$\Delta \bar{C}(g, R) = \lambda \lim_{L \rightarrow \infty} \partial_L \left\langle \exp \left[- (g/\lambda) \int dt \tilde{h}(0, t) \right] h(\mathbf{r}, L) \right\rangle. \tag{4.41}$$

The two series are related term by term via the mapping (4.17) [45]:

$$(\beta\lambda)^{m-1} \overline{\langle \Phi(t_1) \cdots \Phi(t_N) \rangle^c} = \lim_{L \rightarrow \infty} \langle \tilde{h}(0, t_1) \cdots \tilde{h}(0, t_N) h(\mathbf{r}, L) \rangle. \tag{4.42}$$

Equation (3.38) translates into an operator product expansion for the ghost fields:

$$\tilde{h}(\mathbf{r}, t)\tilde{h}(\mathbf{r}', t') = \lambda C |t - t'|^{-(\chi+d)/z} \mathcal{H}\left(\frac{|t - t'|}{|\mathbf{r} - \mathbf{r}'|^z}\right) \tilde{h}(\mathbf{r}, t) \tag{4.43}$$

which produces an equal-time singularity $\tilde{h}(\mathbf{r}, t)\tilde{h}(\mathbf{r}', t) \sim |\mathbf{r} - \mathbf{r}'|^{-(\chi+d)} \tilde{h}(\mathbf{r}, t)$. It is quite plausible intuitively that the response to a pair of nearby sources reduces to the response to a single source multiplied by a divergent factor. This form of the operator product expansion follows also from the mode-coupling approach of [76].

4.5. Height correlations in the strong-coupling regime

In the following, we discuss the renormalized and connected equal-time height correlations

$$\langle h(\mathbf{r}_1, t) \cdots h(\mathbf{r}_n, t) \rangle \equiv \langle h(\mathbf{r}_1) \cdots h(\mathbf{r}_n) \rangle_t \tag{4.44}$$

in the strong-coupling regime, following [49]. An infinite surface growing from a flat initial state $h(\mathbf{r}, 0) = 0$ develops height correlations depending on the differences $\mathbf{r}_{ij} \equiv \mathbf{r}_i - \mathbf{r}_j$ and the correlation length $\xi_t \sim t^{1/z}$ increasing with time. (In a finite system of size R , the correlation length will eventually saturate at a value $\xi \sim R$. We restrict ourselves here to unsaturated growth, i.e., to values $R \gg \xi_t$.) In the scaling regime

$$\tilde{r} \ll |\mathbf{r}_{ij}| \ll \xi_t \quad (i, j = 1, \dots, n) \tag{4.45}$$

the height correlations will generically become singular as some of the points approach each other. For $d < d_s$, these singularities should be power laws. They are assumed to follow from an operator product expansion

$$h(\mathbf{r}_1) \cdots h(\mathbf{r}_k) = \sum_{\mathcal{O}} |\mathbf{r}_{12}|^{-kx_h + x_{\mathcal{O}}} C_k^{\mathcal{O}}\left(\frac{\mathbf{r}_{13}}{|\mathbf{r}_{12}|}, \dots, \frac{\mathbf{r}_{1k}}{|\mathbf{r}_{12}|}\right) \mathcal{O}(\mathbf{r}_1) \tag{4.46}$$

which is an identity expressing any n -point function as a sum of $(n - k + 1)$ -point functions in the limit $|\mathbf{r}_{ij}| \ll |\mathbf{r}_{il}| \ll \xi_t$ ($i, j = 1, \dots, k$ and $l = k + 1, \dots, n$). The sum on the r.h.s. runs over all local scaling fields $\mathcal{O}(\mathbf{r})$. Each term contains a dimensionless scaling function $C_k^{\mathcal{O}}$ (a simple number for $k = 2$) and a power of $|\mathbf{r}_{12}|$ given by the scaling dimensions $x_{\mathcal{O}}$ and $x_h = -\chi$ (such that the overall dimension equals that of the l.h.s.). The field \mathcal{O}_k with the smallest dimension, x_k , determines in particular the asymptotic behaviour of the k -point functions as $\xi_t \rightarrow \infty$,

$$\langle h(\mathbf{r}_1) \cdots h(\mathbf{r}_k) \rangle_t \sim \langle \mathcal{O}_k \rangle_t \sim \xi_t^{-x_k}. \tag{4.47}$$

The amplitudes $\langle \mathcal{O}_k \rangle_t = \langle \mathcal{O}_k(\mathbf{r}) \rangle_t$ diverge with ξ_t , i.e., $x_k < 0$. They measure the global roughness, which increases as the surface develops higher mountains and deeper valleys. Local properties of the surface should, however, behave quite differently. For example, the gradient correlation functions are assumed to have a finite limit:

$$\lim_{\xi_t \rightarrow \infty} \langle \nabla h(\mathbf{r}_1) \cdots \nabla h(\mathbf{r}_n) \rangle_t \equiv \langle \nabla h(\mathbf{r}_1) \cdots \nabla h(\mathbf{r}_n) \rangle. \tag{4.48}$$

On writing

$$h(\mathbf{r}_i) - h(\mathbf{r}'_i) = \int_{\mathbf{r}_i}^{\mathbf{r}'_i} d\mathbf{s} \cdot \nabla h(\mathbf{s})$$

the same property follows for the height difference correlation functions

$$\langle (h(\mathbf{r}_1) - h(\mathbf{r}'_1)) \cdots (h(\mathbf{r}_n) - h(\mathbf{r}'_n)) \rangle_t. \tag{4.49}$$

This implies a feature familiar from simulations: one cannot recognize the value of ξ_t from snapshots of the surface in a region much smaller than ξ_t .

The stationarity condition (4.48) severely restricts the form of the height correlations (4.44). This can be seen as follows. The operator product expansion (4.46) induces an expansion for the gradient field $\mathbf{v} \equiv \nabla h$ of the form

$$\mathbf{v}(\mathbf{r}_1) \cdots \mathbf{v}(\mathbf{r}_k) = \sum_{\mathcal{O}} |\mathbf{r}_{12}|^{-kx_v+x_{\mathcal{O}}} \tilde{C}_k^{\mathcal{O}} \left(\frac{\mathbf{r}_{13}}{|\mathbf{r}_{12}|}, \dots, \frac{\mathbf{r}_{1k}}{|\mathbf{r}_{12}|} \right) \mathcal{O}(\mathbf{r}_1) \quad (4.50)$$

with new scaling functions $\tilde{C}_k^{\mathcal{O}}$ and the dimension $x_v = -\chi + 1$. (Both sides of (4.50) are tensors of rank k whose indices are suppressed.) The fields \mathcal{O} on the r.h.s. govern the time-dependent amplitudes $\langle \mathbf{v}(\mathbf{r}_1) \cdots \mathbf{v}(\mathbf{r}_k) \rangle_t \sim \langle \mathcal{O} \rangle_t \sim \xi_t^{-x_{\mathcal{O}}}$ in analogy with (4.47). Hence, the stationarity condition (4.48) allows in (4.50) only fields \mathcal{O} with a *non-negative* scaling dimension $x_{\mathcal{O}}$, such as $\mathbf{1}$ (the identity field), $(\nabla h)^2(\mathbf{r})$, etc. This in turn restricts the possible terms in (4.46) to the following.

(a) *Singular* terms involving fields $\mathcal{O}(\mathbf{r})$ with $x_{\mathcal{O}} \geq 0$. In particular, we call the coefficient function of $\mathbf{1}$ the *contraction* of the fields $h(\mathbf{r}_1), \dots, h(\mathbf{r}_k)$.

(b) *Regular* terms, where the coefficient $|\mathbf{r}_{12}|^{-kx_h+x_{\mathcal{O}}} C_k^{\mathcal{O}}$ is a tensor of rank N in the differences \mathbf{r}_{1i} ($i = 2, \dots, k$). Such terms do not violate (4.48) since they have a vanishing coefficient $\tilde{C}_k^{\mathcal{O}}$ in (4.50) for $N < k$. They can readily be associated with composite fields of dimensions

$$x_{k,N} = -k\chi + N. \quad (4.51)$$

The leading ($N = 0$) term involves the (normal-ordered) field $\mathcal{O}_k(\mathbf{r}) = h^k(\mathbf{r})$ and governs the asymptotic singularity (4.47) with $x_k = x_{k,0} = -k\chi$. The higher terms correspond to fields with k factors $h(\mathbf{r})$ and N powers of ∇ .

The leading terms of (4.46) are shown in figure 8.

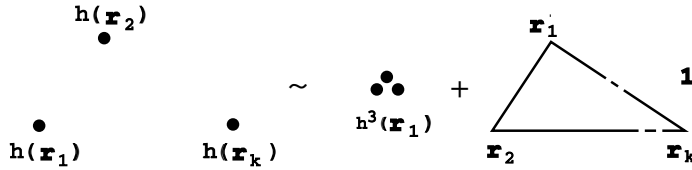


Figure 8. The operator product expansion for a k -tuple of KPZ height fields. The lines indicate the contraction of the fields, i.e., the coupling to the identity $\mathbf{1}$. Partial contractions would not contribute to connected correlation functions. Subleading singular and regular terms are omitted.

It is useful to introduce the (normal-ordered) vertex fields

$$Z_q(\mathbf{r}) \equiv \exp[qh(\mathbf{r})] \quad (4.52)$$

which are the generating functions of the fields $h^k(\mathbf{r})$. Equation (4.46) then implies the operator product expansion

$$Z_{q_1}(\mathbf{r}_1)Z_{q_2}(\mathbf{r}_2) = \exp\left(\sum_{k,l} C_{k,l}^{\mathbf{1}} w_1^k w_2^l\right) Z_{q_1+q_2}(\mathbf{r}_1) + O(C_{k,l}^{\mathcal{O} \neq \mathbf{1}}) \quad (4.53)$$

where $C_{k,l}^{\mathcal{O}} \equiv C_{k+l}^{\mathcal{O}}(0, \dots, 0, \mathbf{r}_{12}/|\mathbf{r}_{12}|, \dots, \mathbf{r}_{12}/|\mathbf{r}_{12}|)$ with the first k arguments equal to 0 and $w_i \equiv q_i |\mathbf{r}_{12}|^\chi$ [95]. This is a generalization of Wick's theorem. In an expansion of the exponential, each term $C_{k,l}^{\mathbf{1}} w_1^k w_2^l$ represents a contraction of $k + l$ fields h . Subleading

singular terms (with positive-dimensional fields \mathcal{O}) and regular terms (with fields containing height gradients) are omitted. Equation (4.53) determines the asymptotic behaviour of the vertex n -point functions:

$$\langle Z_{q_1}(\mathbf{r}_1) \cdots Z_{q_n}(\mathbf{r}_n) \rangle_t \sim \exp\left(\xi_t^\chi \sum_{i=1}^n q_i\right). \tag{4.54}$$

If $\sum_i q_i = 0$, they have a finite limit $\langle Z_{q_1}(\mathbf{r}_1) \cdots Z_{-q_1 \cdots -q_{n-1}}(\mathbf{r}_n) \rangle$. Since these are precisely the vertex correlators that generate the height difference correlation functions (4.49) and since the vertex operator product expansion is analytic in the q_i , this leads back to the stationarity condition (4.48).

The operator product expansions (4.46) and (4.53) with the linear dimensions (4.51) are at the heart of the field theory for KPZ systems. They describe the following structure of height correlations.

(a) The single-point amplitudes

$$\langle h^k \rangle_t \sim \xi_t^{k\chi} \tag{4.55}$$

are the moments of a probability distribution,

$$\langle h^k \rangle_t = \int dh h^k P_{1,t}(h). \tag{4.56}$$

The time dependence of the distribution takes the form

$$P_{1,t}(h) = \xi_t^{-\chi} \mathcal{P}_1(h \xi_t^{-\chi}) \tag{4.57}$$

expressing global scaling of unsaturated growth. Recall that by normal ordering equation (1.1), we have eliminated the non-universal part of the average height, $\langle h \rangle_t \sim t$.

(b) Since (4.46) does not have singular terms with negative-dimensional operators, the local correlation functions (4.48) and (4.49) decouple from the global amplitudes (4.55). In particular, powers of the height difference $h_{12} \equiv h(\mathbf{r}_1) - h(\mathbf{r}_2)$ reach stationary expectation values for $\xi_t \rightarrow \infty$ determined by the contraction term in (4.46),

$$\langle h_{12}^k \rangle \sim |\mathbf{r}_{12}|^{k\chi}. \tag{4.58}$$

These can be written as moments of a stationary probability distribution

$$\langle h_{12}^k \rangle = \int dh_{12} h_{12}^k P_2(h_{12}, |\mathbf{r}_{12}|) \tag{4.59}$$

which has the scaling form

$$P_2(h_{12}, r) = r^{-\chi} \mathcal{P}_2(h_{12} r^{-\chi}). \tag{4.60}$$

Equation (4.58) can be verified exactly for $d = 1$ and seems to be consistent with the currently available numerical data also for higher dimensions.

It is instructive to compare this structure with models of turbulence. Burgers' equation (1.4) with force correlations

$$\overline{\eta(\mathbf{r}, t) \eta(\mathbf{r}', t')} = \varepsilon r_0^2 \delta(t - t') \Delta \left(\frac{|\mathbf{r} - \mathbf{r}'|}{r_0} \right) \tag{4.61}$$

over large distances r_0 develops *multiscaling*: for example, the longitudinal velocity difference moments

$$\langle [v_{\parallel}(\mathbf{r}_1) - v_{\parallel}(\mathbf{r}_2)]^k \rangle \sim |\mathbf{r}_{12}|^{-k\chi_v + \tilde{\chi}_k} r_0^{-\tilde{\chi}_k} \tag{4.62}$$

have a k -dependent singular dependence on $|\mathbf{r}_{12}|$ and r_0 for

$$r_0/\mathcal{R} \ll |\mathbf{r}_{12}| \ll r_0 \tag{4.63}$$

where $\mathcal{R} \equiv r_0^{4/3} \varepsilon^{1/3} / \nu$ denotes the Reynolds number [96, 35]. This so-called inertial scaling regime should be compared to the KPZ strong-coupling regime $\tilde{r} \ll |r_{12}| \ll \xi_t$. According to (4.62) local and global scaling properties are no longer decoupled. Similar multiscaling is present in Navier–Stokes turbulence. Kolmogorov’s famous argument predicts the exact scaling dimension of the velocity field, $x_v = -1/3$, from dimensional analysis [97]. This determines the scaling of the third moment in (4.62) since $\tilde{x}_3 = 0$. The higher exponents $\tilde{x}_4, \tilde{x}_5, \dots < 0$ cannot be obtained from dimensional analysis. Assuming the existence of an operator product expansion (4.50), the term (4.62) is generated by the lowest-dimensional field \tilde{O}_k with a singular coefficient. A similar operator product expansion is discussed in [98]. Multiscaling thus implies the existence of a (presumably infinite) number of composite fields with anomalous negative dimensions. For the velocity vertex fields $\exp[qv(r)]$ of Burgers turbulence in one dimension, Polyakov has conjectured an operator product expansion similar to (4.53) [99]. The distinguishing feature of KPZ surfaces is the absence of multiscaling expressed by (4.48).

4.6. The dynamical anomaly and quantized scaling

The operator product expansion (4.53) and the dispersion relation (4.51) have to be consistent with the underlying dynamics (4.7). However, as explained in [99] for Burgers turbulence, the equation of motion for the renormalized correlation functions is quite subtle due to anomalies dictated by the operator product expansion. To exhibit the anomalies for the height correlations [49], we introduce the smeared vertex fields

$$Z_q^a(\mathbf{r}) \equiv \exp\left(q \int d\mathbf{r}' \delta_a(\mathbf{r} - \mathbf{r}') h(\mathbf{r}')\right) \tag{4.64}$$

(where $\delta_a(\mathbf{r})$ is a normalized function with support in the sphere $|\mathbf{r}| < a$) and the abbreviations $Z_i^a \equiv Z_{q_i}^a(\mathbf{r}_i)$, $Z_i \equiv Z_{q_i}(\mathbf{r}_i)$.

Using (4.6) and (4.7), it is straightforward to derive the equation of motion

$$\partial_t \langle Z_1^a \cdots Z_n^a \rangle_t = \sum_{i=1}^n q_i \langle Z_1^a \cdots \mathcal{J} Z_i^a \cdots Z_n^a \rangle_t \tag{4.65}$$

where

$$\mathcal{J} Z_i^a \equiv [q_i \sigma^2 \delta_a(0) + J(\mathbf{r}_i)] Z_i^a. \tag{4.66}$$

The singularity structure of the current is determined by (4.46) and (4.36):

$$\mathcal{J} Z_i^a = g^* \hat{Z}_i + a^{2\chi-2} \left(\sum_{k=1}^{\infty} c_k a^{k\chi} q_i^k \right) Z_i + O(a^\chi) \tag{4.67}$$

for $a, \tilde{r} \rightarrow 0$ with a/\tilde{r} kept constant. The field $\hat{Z}_q(\mathbf{r}) \equiv (\nabla h)^2 Z_q(\mathbf{r})$ denotes the finite part of the operator product $(\nabla h)^2(\mathbf{r}) Z_q^a(\mathbf{r})$ for $a \rightarrow 0$, and $\hat{Z}_i \equiv \hat{Z}_{q_i}(\mathbf{r}_i)$. The finite dissipation term $(\nabla^2 h) Z_{q_i}(\mathbf{r}_i)$ becomes irrelevant in this limit since $\nu \sim a^\chi$. The singular part of (4.67) is a power series in q_i with asymptotically constant coefficients

$$\begin{aligned} c_1 &= \sigma^{*2} a^d \delta_a(0) + \nu^* c_{1,1} + g^* c_{2,1} \\ c_k &= \nu^* c_{1,k} + g^* c_{2,k} \quad (k = 2, 3, \dots). \end{aligned}$$

The terms of order $a^{(2+k)\chi-2}$ originate from the contractions $\nabla^2 h(\mathbf{r}_i) h(\mathbf{r}'_1) \cdots h(\mathbf{r}'_k) \sim \mathbf{1}$ and $(\nabla h)^2(\mathbf{r}_i) h(\mathbf{r}'_1) \cdots h(\mathbf{r}'_k) \sim \mathbf{1}$. (Their respective coefficients $c_{1,k}$ and $c_{2,k}$ are complicated integrals involving the scaling functions in (4.46), the regularizing functions $\delta_a(\mathbf{r}_i - \mathbf{r}'_j)$,

and the ratio a/\tilde{r} .) Of course, divergent terms have to cancel so that equation (4.65) has a finite continuum limit:

$$\partial_t \langle Z_1 \cdots Z_n \rangle_t = \sum_{i=1}^n q_i \langle Z_1 \cdots \mathcal{J} Z_i \cdots Z_n \rangle_t \tag{4.68}$$

with

$$\mathcal{J} Z_i = \lim_{a \rightarrow 0} \mathcal{J} Z_i^a. \tag{4.69}$$

For generic values of χ , this implies that $\mathcal{J} Z_i = g^* \hat{Z}_i$. However, if χ satisfies the condition (4.1) for some integer k_0 , the dissipation current contributes an anomaly:

$$\mathcal{J} Z_i = g^* \hat{Z}_i + v^* c_{1,k_0} q_i^{k_0} Z_i. \tag{4.70}$$

Equations (4.68) and (4.70) govern in particular the stationary state of the surface. For $d = 1$, the stationary height distribution $P[h]$ is known:

$$P \sim \exp\left(-\frac{\sigma^2}{\nu} \int dr (\nabla h)^2\right). \tag{4.71}$$

It equals that of the linear theory, thus restoring the up-down symmetry $h(\mathbf{r}) - \langle h \rangle_t \rightarrow -h(\mathbf{r}) + \langle h \rangle_t$ broken by the non-linear term in (1.1). The exponent $\chi = 1/2$ satisfies (4.1) with $k_0 = 2$ but the up-down symmetry forces the anomaly to vanish ($c_{1,2} = 0$). In higher dimensions, this symmetry is expected to remain broken in the stationary regime. The surface has rounded hilltops and steep valleys, just like the upper side of a cumulus cloud (argued in reference [100] to be a KPZ surface). Hence, the local slope of the surface is correlated with the relative height, resulting in non-zero odd moments $\langle (\nabla h)^2(\mathbf{r}_1)[h(\mathbf{r}_1) - h(\mathbf{r}_2)]^k \rangle$. However, this is consistent with equations (4.68) and (4.70) only for odd values of k_0 , where

$$\langle \hat{Z}_q(\mathbf{r}_1) Z_{-q}(\mathbf{r}_2) \rangle - \langle \hat{Z}_{-q}(\mathbf{r}_1) Z_q(\mathbf{r}_2) \rangle = -(v^*/g^*) c_{1,k_0} q^{k_0} \langle Z_q(\mathbf{r}_1) Z_{-q}(\mathbf{r}_2) \rangle \tag{4.72}$$

and hence for odd values of $k \geq k_0$

$$\langle (\nabla h)^2(\mathbf{r}_1)[h(\mathbf{r}_1) - h(\mathbf{r}_2)]^k \rangle = -(v^*/g^*) c_{1,k_0} \langle [h(\mathbf{r}_1) - h(\mathbf{r}_2)]^{k-k_0} \rangle. \tag{4.73}$$

The directedness of the stationary growth pattern thus requires a non-zero anomaly c_{1,k_0} with an odd integer k_0 . The roughness exponent is then determined by equation (4.1). The values $k_0 = 3$ for $d = 2$ and $k_0 = 5$ for $d = 3$ give the exponents (4.74) and (4.75) quoted below. These appear to be consistent with the numerical results $\chi \approx 0.39$ and $\chi \approx 0.31$ [25, 26], respectively, and with the experimental value $\chi = 0.43 \pm 0.05$ for $d = 2$ [33].

4.7. Discussion

The scaling of strongly driven surfaces has been determined by requiring consistency of the effective large-distance field theory subject to a few phenomenological constraints. These are the existence of a local operator product expansion (4.46) and of a stationary state (4.48) that is directed (i.e., has no up-down symmetry). The stationarity condition has an important consequence: the decoupling of local and global scaling properties. The latter can be expressed by the time-dependent height probability distribution at a single point, the former by the stationary distribution of the height difference between nearby points.

The Galilei invariance of the dynamic equation conspires with these constraints to allow only discrete values of the roughness exponent in two and three dimensions:

$\chi = 2/(k_0 + 2)$ with an odd integer k_0 . Comparison with numerical estimates then gives the exact values

$$\chi = 2/5 \quad z = 8/5 \quad \text{for } d = 2 \tag{4.74}$$

and

$$\chi = 2/7 \quad z = 12/7 \quad \text{for } d = 3. \tag{4.75}$$

The underlying solutions of the KPZ equation are distinguished by a dynamical anomaly in the strong-coupling regime: the dissipation term contributes a finite part to the effective equation of motion (4.68) despite being formally irrelevant. The anomaly manifests itself in identities like (4.73) between stationary correlation functions, which can be tested numerically.

There are at least three directions of future research where these concepts and methods can be of use. As mentioned in the introduction, the field of stochastic growth is rather diverse, and the theoretical cousins of the KPZ equation could be analysed in a similar way, aiming at a better understanding of these non-equilibrium universality classes. In contrast to the KPZ equation, some of these systems do show multiscaling [101], which makes their field-theoretic description certainly more complex.

Further applications to the theory of disordered systems are equally important. The present theory should be extendable from a directed string to higher-dimensional manifolds in a random medium.

Finally, this theory highlights both the theoretical similarities and differences of surface growth and fluid turbulence. While it is quite surprising that the scaling exponents of an interacting dynamical field theory can be predicted exactly in two and three dimensions, there is one other such case in a related system: the exact Kolmogorov scaling of the third velocity difference moment in Navier–Stokes turbulence. The higher velocity difference moments show multiscaling (see section 4.5). For the simpler case of Burgers turbulence, dynamical anomalies are intrinsically connected to the multiscaling exponents [102]. This link is expected to be important in a wider context of turbulence.

Perhaps some of these fascinating scaling phenomena far from equilibrium are not as inaccessible as they have appeared so far.

Appendix

This appendix contains some details about the renormalization of the replicated string system (section 3.1) and the dynamic functional (section 4.2).

We start from the replica partition function

$$Z = \int \mathcal{D}\phi \mathcal{D}\bar{\phi} \exp \left[- \int_0^{L_0} dt_0 \int_0^R d\mathbf{r} (\bar{\phi}(\partial_{t_0} - \nabla^2)\phi + g_0 \bar{\phi}^2 \phi^2) \right] \tag{A.1}$$

with the effective coupling constant (3.12), obtained from (3.9) by making the change of variables $t_0 \rightarrow \beta_0^{-1} t_0$. The field ϕ is real valued with the constraint $\phi > 0$; the field $\bar{\phi}$ is purely imaginary [92]. The normal-ordered interaction $g_0 \bar{\phi}^2 \phi^2$ conserves the number of strings. To evaluate (A.1), we take periodic boundary conditions for the components of \mathbf{r} and define

$$Z_p = \langle p, \mathbf{r} | Z | p \rangle \tag{A.2}$$

with the initial state

$$|p\rangle \equiv (1/p!) \left[\int d\mathbf{r} \bar{\phi}(\mathbf{r}) \right]^p |0\rangle$$

at $t_0 = 0$ and the final state

$$\langle p, \mathbf{r} | \equiv \langle 0 | \phi^p(\mathbf{r})$$

at $t_0 = L_0$. Correlation functions $\langle \dots \rangle_p$ are defined in a similar way. With an appropriate normalization of the propagator, these boundary conditions normalize $Z_p(g_0, L_0 = 0, R) = Z_p(g_0 = 0, L_0, R) = 1$ for any value of p .

The Casimir amplitude is defined by analogy with (2.4) and (2.12). Its expansion in terms of the dimensionless coupling $u_0 \equiv g_0 R^{2\gamma_0}$

$$\Delta C_p(u_0) = -R^{-2} \sum_{N=1}^{\infty} \frac{(-g_0)^N}{N!} \int dt_{02} \dots dt_{0N} \langle \Phi_2(0) \Phi_2(t_{02}) \dots \Phi_2(t_{0N}) \rangle_p^c \tag{A.3}$$

is a sum involving connected pair field correlations in the p -string sector of the unperturbed theory ($u_0 = 0$). The integrals in equation (A.3) are infrared regularized by the system width R ; their ultraviolet singularities are determined by the short-distance structure of the pair field correlations and have to be absorbed into the coupling constant renormalization. Hence consider the N -point function $\langle \Phi_2(t_{01}) \dots \Phi_2(t_{0N}) \rangle_p^c$ as the points t_{01}, \dots, t_{0N} approach each other. More precisely, we define t_0 and τ_{jk} by $t_{0j} - t_{0k} = t_0 \tau_{jk}$ and let

$$t_0/R^2 \rightarrow 0 \tag{A.4}$$

with τ_{jk} and the ‘centre of mass’ $t'_0 = N^{-1} \sum_{j=1}^N t_{0j}$ remaining fixed. The asymptotic scaling is given by the p -independent operator product expansion

$$\Phi_2(t_{01}) \dots \Phi_2(t_{0N}) = \sum_{m=2}^{N+1} t_0^{-(N-m+1)d/2} [C_N^m(\tau_1, \dots, \tau_{N-2}) \Phi_m(t'_0) + \dots] \tag{A.5}$$

where the C_N^m are scaling functions of the $N - 2$ linearly independent distance ratios τ_{jk} , the dots denote subleading terms down by positive integer powers of t_0/R^2 , and we have defined the normal-ordered m -string contact fields

$$\Phi_m(t_0) \equiv \int d\mathbf{r} \bar{\phi}^m(\mathbf{r}, t_0) \phi^m(\mathbf{r}, t_0). \tag{A.6}$$

For $m = N = 2$, equation (A.5) reduces to (2.11); i.e., $C_2^2 = C_0$. The operator product expansion dictates the leading singularities of the integrals in (A.3):

$$\begin{aligned} & \int dt_0 t_0^{N-2} \prod_{l=1}^{N-2} d\tau_l \langle \Phi_2(t_{01}) \dots \Phi_2(t_{0N}) \rangle_p \\ &= \sum_{m=2}^{N+1} \int J_N^m t_0^{m-3+\gamma_0(N-m+1)} dt_0 \langle \Phi_m(t'_0) \rangle_p + \dots \end{aligned} \tag{A.7}$$

with

$$J_N^m = \int \prod_{l=1}^{N-2} d\tau_l C_N^m(\tau_1, \dots, \tau_{N-2}). \tag{A.8}$$

The diagrammatic representation of the perturbation series (A.3) is discussed in detail in reference [44]. At any integer value of p , the series is somewhat simplified since

$$\langle \Phi_m \rangle_p = 0 \quad \text{for } m > p. \tag{A.9}$$

For p non-integer, all values of m contribute, e.g., to (A.7). Hence, the series becomes complicated in the random limit $p \rightarrow 0$. Its pole structure at $\gamma_0 = 0$, however, remains simple. Consider the term in (A.5) with $N = m = 2$, corresponding to the diagram of

figure A1(a). The loop has the value $R^{2y_0}c(y_0)/y_0$ with $c(y_0) = C_0(y_0) + O(y_0)$. The pole originates from the universal short-distance singularity in (A.7), while the finite part depends also on the infrared regularization. Hence, we obtain to one-loop order

$$\Delta\mathcal{C}_p(u_0) = -R^d \langle \Phi_2 \rangle_p u_0 \left(1 - \frac{c}{y_0} u_0 \right) + O(y_0^0 u_0^2, u_0^3) \tag{A.10}$$

with $R^d \langle \Phi_2 \rangle_p = p(p-1)/4$. The pole can be absorbed into the definition $u_p = \mathcal{Z}_p u_0$ with the \mathcal{Z} -factor (2.18), which leads to the beta function (2.23) and the field renormalization $\Phi_p = \tilde{\mathcal{Z}}_p \Phi$ with (2.21).

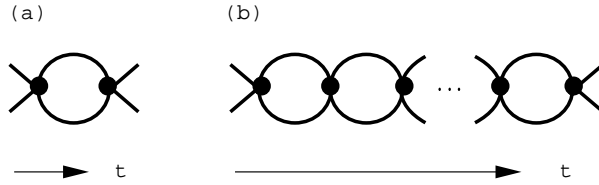


Figure A1. Singular diagrams contributing to the finite-size free energy $\Delta\mathcal{C}_p(u_0)$ in the expansion (A.3). The lines denote unperturbed single-line propagators $\langle \phi(r_1, t_{01})\phi(r_2, t_{02}) \rangle$, the dots pair contact vertices $\Phi_2(t_0)$. (a) A one-loop diagram containing a primitive pole in y_0 . (b) An N -loop diagram containing a pole in y_0 of order $N - 1$.

It is not difficult to discuss higher orders. The ultraviolet singularities of the N th-order integral (A.7) are contained in the coefficients J_N^m or arise from the integration over t_0 . In the first case, they are due to a *proper subdiagram* and hence already absorbed into the renormalized coupling constant at lower order. Only the divergences from the integration over t_0 , with J_N^m denoting the regular part of (A.8), may contribute to the *primitive singularity* at order N . Inspection of (A.7) then shows that a pole at $y_0 = 0$ only appears for $m = 2$. However, there is only one diagram per order of this kind, which is shown in figure A1(b). Since this diagram factorizes into loops of the kind shown in figure A1(a), it contributes a pole in y_0 of order $N - 1$. Therefore the pole at order $N = 2$ is the only primitive singularity in the series (A.3) for the free energy; analogous arguments apply to the expansions of the contact-field correlation functions. It follows that the renormalization can be carried out to all orders; see also references [59, 60]. The loops of figure A1 form a geometric series. Summing this series defines the \mathcal{Z} -factors [43]

$$\mathcal{Z}_p = 1 - \frac{c}{y_0} u_p \quad \tilde{\mathcal{Z}}_p = \frac{du_0}{du_p} = \left(1 - \frac{c}{y_0} u_p \right)^{-2} \tag{A.11}$$

and the flow equation $\dot{u}_p = y_0 u_p - c u_p^2$. The Casimir amplitude $\Delta\mathcal{C}_p$ becomes a regular function of u_p :

$$\Delta\mathcal{C}_p(u_p) = \frac{p(p-1)}{4} u_p + O(u_p^2). \tag{A.12}$$

The coupling u_p defined by (A.11) is not unique. Any family of diffeomorphisms $u_p \rightarrow u'_p(u_p, y_0)$ with fixed point $u'_p(0, y_0) = 0$ will preserve the regular functional dependence of observables such as (A.12). In particular, the linear transformation $u_p \rightarrow (c/C_0)u_p$ leads to the flow equation (2.24) and the \mathcal{Z} -factors

$$\mathcal{Z}_p = \frac{c}{C_0} \left(1 - \frac{C_0}{y_0} u_p \right) \quad \tilde{\mathcal{Z}}_p = \frac{C_0^2}{c^2} \left(1 - \frac{C_0}{y_0} u_p \right)^{-2}. \tag{A.13}$$

We may also substitute $C_0(y_0 = 0)$ for $C_0(y_0)$ in (A.13) and (2.24) so that the dependence of the flow equation on y_0 is contained only in the linear term. This scheme has been called ‘minimal subtraction’ in reference [18]. However, the \mathcal{Z} -factors (A.13) still have a regular part as $y_0 \rightarrow 0$ generated by the function $c(y_0)$. Eliminating this part requires a non-linear transformation of u_p and introduces cubic and higher-order terms into the flow equation [91]. Of course, these terms are spurious; i.e., they do not generate higher-order terms in expressions like (2.25) for local observables. (In the present case of a single coupling constant u_p , the value of the C_0 drops out of these expressions as well. In more general cases with several coupling constants, ratios of operator product coefficients do play a role; see the discussion in reference [1].)

The replica trick is unproblematic within perturbation theory, since it reduces to convenient bookkeeping of the averaging over disorder. Equations (A.13), (2.24) are independent of p , and in equation (A.12), the dependence on p reduces to the combinatoric prefactor. Hence, the random limit $\Delta\bar{C} = \lim_{p \rightarrow 0} C_p/p$ is trivial and leads to equations (3.13) and (3.14).

The exponents (3.15) can also be obtained in a different way. They follow from the fact that the two-string interaction $\bar{\phi}^2\phi^2$ does not renormalize the ‘mass term’ $\bar{\phi}\phi$ at any order. Consider the (normal-ordered) density field $\Phi(t_0) \equiv \bar{\phi}\phi(\mathbf{r} = 0, t_0)$, which has the two-point function

$$\langle \Phi(t_0)\Phi(t'_0) \rangle_p^c(u_0, R) = \sum_{N=0}^{\infty} \frac{(-g_0)^N}{N!} \int dt_{01} \cdots dt_{0N} \langle \Phi(t_0)\Phi(t'_0)\Phi_2(t_{01}) \cdots \Phi_2(t_{0N}) \rangle_p^c. \tag{A.14}$$

Its short-distance asymptotics is related to the probability of strings returning to the origin $\mathbf{r} = 0$. In the linear theory,

$$\langle \Phi(t_0)\Phi(t'_0) \rangle_p^c \sim |t_0 - t'_0|^{-d\zeta_0} \tag{A.15}$$

for $|t_0 - t'_0|/R^2 \ll 1$. Any perturbative correction to this exponent arises from the renormalization of the fields $\Phi(t_0)$ and $\Phi(t'_0)$. The renormalization of $\Phi(t_0)$ is due to a short-distance coupling of the form

$$\Phi(t_0)\Phi_2(t_{01}) \cdots \Phi_2(t_{0N}) = t_0^{-Nd/2} C_N^1(\tau_1, \dots, \tau_{N-1})\Phi(t_0) + \cdots \tag{A.16}$$

for $t_0/R^2 \rightarrow 0$ (with $t_{0j} - t = t_0\tau_j$, $t_{0j} - t_{0k} = t_0\tau_{jk}$ for $j, k = 1, \dots, N$, and $\tau_1, \dots, \tau_{N-1}$ denoting a basis of the fixed ratios τ_j, τ_{jk}), and there is a corresponding expression for $\Phi(t'_0)$. However, it is obvious that the product on the l.h.s. couples only to contact fields of at least two lines, and therefore $C_N^1 = 0$ at all orders N . The singularity (A.15) remains unchanged, $\zeta^* = \zeta_0 = 1/2$. The strong-coupling form (3.37) of the singularity cannot be reached by perturbation theory.

Now we turn to the dynamic path integral. After one makes the change of variables $t_0 \rightarrow \nu_0 t_0$, $h_0 \rightarrow (\nu_0/\sigma_0^2)^{1/2} h_0$, and $\tilde{h}_0 \rightarrow (\sigma_0^2/\nu_0)^{1/2} \tilde{h}_0$, equation (4.3) takes the normal form

$$Z = \int \mathcal{D}h_0 \mathcal{D}\tilde{h}_0 \exp \left[- \int d\mathbf{r} dt \left(-\frac{1}{2} \tilde{h}_0^2 + \tilde{h}_0 \left(\partial_t h_0 - \frac{1}{2} \nabla^2 h_0 - \frac{\lambda_0}{2} (\nabla h_0)^2 \right) \right) \right] \tag{A.17}$$

with $\lambda_0^2 = -g_0$. As discussed in reference [92], the transformation (4.17) leads back to (A.1), rendering dynamical perturbation theory identical to replica perturbation theory. The path integral (A.1) has to be supplemented with boundary conditions corresponding to the random limit $p \rightarrow 0$. In this limit, the boundary condition (A.2) describes the one-point function of an initially flat surface, $\langle h(\mathbf{r}, t_0 = 0) \rangle = 0$. At any integer value of p , the

dynamical correlations are artificially truncated: $\langle \tilde{h}(\mathbf{r}_1, t) \cdots \tilde{h}(\mathbf{r}_m, t) h(\mathbf{r}, L) \rangle_p = 0$ for all $m > p$ by (A.9).

In the context of growth dynamics, the representation (A.17) has an advantage over (A.1): it contains explicitly the most interesting observable, the height field h . The price to pay is that the perturbation theory becomes more complicated. The differences from replica perturbation theory are twofold: (i) there is the cubic vertex $\tilde{h}(\nabla h)^2$; (ii) the vertex \tilde{h}^2 , the image of the replica interaction $\tilde{\phi}^2 \phi^2$, no longer has incoming lines. These vertices can therefore be integrated out, giving the standard diagrammatics with the two kinds of propagator (4.9) and (4.10).

We now discuss the renormalization of (A.17) and show its equivalence to replica renormalization up to one-loop order. The real-space response function has the diagrammatic expansion shown in figure A2(a). To order u_0^2 , the expansion reads

$$R^d \langle \tilde{h}_0(\mathbf{r}, t_0) h_0(\mathbf{r}, t_0 + R^2) \rangle(u_0) = R^d \langle \tilde{h}_0(\mathbf{r}, t_0) h_0(\mathbf{r}, t_0 + R^2) \rangle(0) + O(y_0^0 u_0, u_0^2). \quad (\text{A.18})$$

The one-loop diagram does not have a pole at $d = 2$ since its short-distance singularity cancels with a geometric factor $2 - d$ [90, 17, 91]. Constructing the strong-coupling fixed point for $d = 1$ requires taking into account the resulting finite renormalization of the response function [17]. For the critical fixed point above $d = 2$, however, it can be ignored.

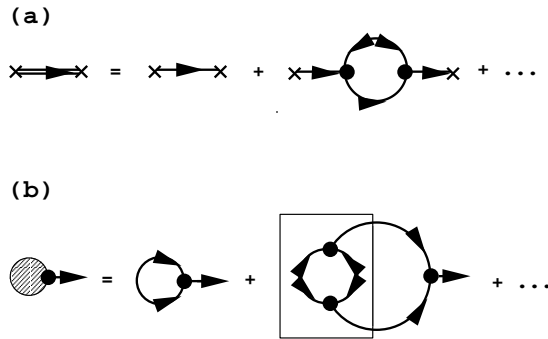


Figure A2. Diagrammatic expansions generated by the dynamic functional (4.3). The lines with one and two arrows denote the unperturbed response function (4.9) and the unperturbed correlation function (4.10), respectively. Dots represent the vertices $\tilde{h}(\nabla h)^2$; each incoming line to a vertex has to be differentiated with respect to \mathbf{r} . (a) The response function $\langle \tilde{h}(\mathbf{r}_1, t_{01}) h(\mathbf{r}_2, t_{02}) \rangle$. The one-loop diagram is regular at $y_0 = 0$. (b) The stationary growth rate $\langle \partial_{t_0} h_0 \rangle_R$. The boxed subdiagram contains a simple pole at $y_0 = 0$. A further diagram with a loop like that in (a) is regular at $y_0 = 0$ and has been omitted.

The expansion for the growth velocity is shown in figure A2(b). The tadpole diagram at order λ_0 has the form

$$\lambda_0 \left[I(R) - \lim_{R \rightarrow \infty} I(R) \right] = -\frac{\lambda_0}{2} R^{-d} \quad (\text{A.19})$$

with

$$I(R) = \int d\mathbf{r}' dt'_0 [\nabla_{\mathbf{r}} \langle \tilde{h}_0(\mathbf{r}', t'_0) h(\mathbf{r}, t) \rangle_R(u_0 = 0)]^2. \quad (\text{A.20})$$

The second term in (A.19) is generated by the normal ordering (4.15) and cancels the ultraviolet divergence of $I(R)$. At order λ_0^3 , the boxed subdiagram contributes a pole

originating from the integration region where the two vertices approach each other. Hence, we have to this order

$$R^{2-\chi_0} \langle \partial_{t_0} h_0 \rangle_R(u_0) = -\frac{1}{2} u_0^{1/2} \left(1 - \frac{C_0}{y_0} u_0 + O(y_0^0 u_0, u_0^2) \right). \quad (\text{A.21})$$

The pole can be absorbed into the definition of the variables $h_P = \mathcal{Z}_{Ph} h_0$, $\tilde{h}_P = \mathcal{Z}_{Ph}^{-1} \tilde{h}_0$, $t_P = \mathcal{Z}_{Pt} t_0$, $u_P = \mathcal{Z}_P u_0$, with

$$\mathcal{Z}_{Ph}(u_P) = 1 + \frac{C_0}{2y_0} u_P + O(u_P^2) \quad (\text{A.22})$$

$$\mathcal{Z}_{Pt}(u_P) = 1 + O(u_P^2) \quad (\text{A.23})$$

$$\mathcal{Z}_P(u_P) = 1 - \frac{C_0}{y_0} u_P + O(u_P^2). \quad (\text{A.24})$$

This reparametrization respects (4.25) and renders both the response function and the growth rate regular as $y_0 \rightarrow 0$:

$$R^d \langle \tilde{h}_P(\mathbf{r}, t_P) h_P(\mathbf{r}, t_P + R^2) \rangle(u_P) = R^d \langle \tilde{h}_0(\mathbf{r}, t_0) h_0(\mathbf{r}, t_0 + R^2) \rangle(0) + O(y_0^0 u_P, u_P^2) \quad (\text{A.25})$$

$$R^{2-\chi_0} \langle \partial_{t_P} h_P \rangle_R(u_P) = -\frac{1}{2} u_P^{1/2} (1 + O(y_0^0 u_P, u_P^2)). \quad (\text{A.26})$$

It leads to the beta function (2.23) and to the exponents

$$\chi^* = 2 - z^* = \chi_0 - \dot{u}_P \left. \frac{d}{du_P} \log \mathcal{Z}_{Ph}(u_P) \right|_{u_P^*} = O(y_0^2). \quad (\text{A.27})$$

Acknowledgments

This article is an extended version of my habilitation thesis (University of Potsdam, 1997). I wish to express my warmest thanks to Reinhard Lipowsky for support and encouragement. Sections 3.2, 3.3, 3.5, 3.6 and 4.4 result from a very enjoyable collaboration with Harald Kinzelbach. Many people have generously shared their insights with me; I am grateful in particular to Ralf Bundschuh, John L Cardy, Christin Hiergeist, Terence Hwa, Harald Kallabis, Harald Kinzelbach, Thomas Nattermann, Reinhard Lipowsky, Lei-Han Tang, Karen Willbrand and Dietrich Wolf.

References

- [1] Cardy J L 1996 *Scaling and Renormalization in Statistical Physics* (Cambridge: Cambridge University Press)
- [2] Itzykson C and Drouffe J-M 1989 *Statistical Field Theory* vol 2 (Cambridge: Cambridge University Press)
- [3] Krug J and Spohn H 1990 *Solids Far From Equilibrium* ed C Godrèche (Cambridge: Cambridge University Press)
- [4] Halpin-Healy T and Zhang Y-C 1995 *Phys. Rep.* **254** 215
- [5] Herrasti P, Ocon P, Salvarezza R C, Vara J M and Arvia A J 1992 *Phys. Rev. A* **45** 7440
- [6] Kahanda G, Zon X, Farrell R and Wong P 1992 *Phys. Rev. Lett.* **68** 3741
- [7] Bak P, Chen K and Tang C 1990 *Phys. Lett.* **147A** 297
- [8] Drossel B and Schwabl F 1992 *Phys. Rev. Lett.* **69** 1629
- [9] Kardar M, Parisi G and Zhang Y C 1986 *Phys. Rev. Lett.* **56** 889
- [10] Wolf D and Villain J 1990 *Europhys. Lett.* **13** 389
- [11] Krug J 1995 *Scale Invariance, Interfaces and Non-Equilibrium Dynamics* ed A McKane *et al* (New York: Plenum)

- [12] Imbrie J Z and Spencer T 1988 *J. Stat. Phys.* **52** 609
- [13] Cook J and Derrida B 1989 *Europhys. Lett.* **10** 195
Cook J and Derrida B 1990 *J. Phys. A: Math. Gen.* **23** 1523
- [14] Evans M R and Derrida B 1992 *J. Stat. Phys.* **69** 427
- [15] Tang L-H, Nattermann T and Forrest B M 1990 *Phys. Rev. Lett.* **65** 2422
- [16] Nattermann T and Tang L-H 1992 *Phys. Rev. A* **45** 7156
- [17] Frey E and Täuber U C 1994 *Phys. Rev. E* **50** 1024
- [18] Lässig M 1995 *Nucl. Phys. B* **448** 559
- [19] Forster D, Nelson D R and Stephen M 1977 *Phys. Rev. A* **16** 732
- [20] Gwa L-H and Spohn H 1992 *Phys. Rev. Lett.* **68** 725
- [21] Kim J M and Kosterlitz J M 1989 *Phys. Rev. Lett.* **62** 2289
- [22] Forrest B M and Tang L-H 1990 *Phys. Rev. Lett.* **64** 1405
- [23] Kim J M, Kosterlitz J M and Ala-Nissila T 1991 *J. Phys. A: Math. Gen.* **24** 5569
- [24] Kim J M, Moore M A and Bray A J 1991 *Phys. Rev. A* **44** 2345
- [25] Tang L-H, Forrest B M and Wolf D E 1992 *Phys. Rev. A* **45** 7162
- [26] Ala-Nissila T, Hjelt T, Kosterlitz J M and Venäläinen O 1993 *J. Stat. Phys.* **72** 207
- [27] Ala-Nissila T 1998 *Phys. Rev. Lett.* **80** 887
- [28] Kim J M 1998 *Phys. Rev. Lett.* **80** 888
- [29] Halpin-Healy T 1989 *Phys. Rev. Lett.* **62** 445
Halpin-Healy T 1990 *Phys. Rev. A* **42** 711
- [30] Nattermann T and Leschhorn H 1991 *Europhys. Lett.* **14** 603
- [31] Moore M A, Blum T, Doherty J P, Marsili M, Bouchaud J P and Claudin P 1995 *Phys. Rev. Lett.* **74** 4257
and references therein
- [32] Maunuksela J, Myllys M, Timonen J, Alava M J and Ala-Nissila T 1998 *Preprint*
- [33] Paniago R, Forrest R, Chow P C, Moss S C, Parkin S and Cookson D 1997 *Phys. Rev. B* **56** 13 442
- [34] Meakin P, Ramanlal P, Sander L M and Ball R C 1986 *Phys. Rev. A* **34** 3390
- [35] Bouchaud J P, Mézard M and Parisi G 1995 *Phys. Rev. E* **52** 3656
- [36] Huse D A and Henley C L 1985 *Phys. Rev. Lett.* **54** 2708
- [37] Kardar M 1985 *Phys. Rev. Lett.* **55** 2235
Kardar M 1987 *Nucl. Phys. B* **290** 582
- [38] Fisher D S and Huse D A 1991 *Phys. Rev. B* **43** 10728
- [39] Frey E, Täuber U C and Hwa T 1996 *Phys. Rev. E* **53** 4424
- [40] Forgacs G, Lipowsky R and Nieuwenhuizen T M 1991 *Phase Transitions and Critical Phenomena* vol 14,
ed C Domb and J L Lebowitz (London: Academic)
- [41] Lässig M and Lipowsky R 1993 *Phys. Rev. Lett.* **70** 1131
- [42] Lässig M 1994 *Phys. Rev. Lett.* **73** 561
- [43] Lässig M and Lipowsky R 1994 *Fundamental Problems of Statistical Mechanics VIII* (Amsterdam: Elsevier)
- [44] Bundschuh R and Lässig M 1996 *Phys. Rev. E* **54** 304
- [45] Kinzelbach H and Lässig M 1995 *J. Phys. A: Math. Gen.* **28** 6535
- [46] Kinzelbach H and Lässig M 1995 *Phys. Rev. Lett.* **75** 2208
- [47] Lässig M and Kinzelbach H 1997 *Phys. Rev. Lett.* **78** 903
- [48] Lässig M and Kinzelbach H 1998 *Phys. Rev. Lett.* **80** 889
- [49] Lässig M 1998 *Phys. Rev. Lett.* **80** 2366
- [50] Jayaprakash C, Rottmann C and Saam W F 1984 *Phys. Rev. B* **30** 6549
- [51] Nelson D R 1988 *Phys. Rev. Lett.* **60** 1973
Nelson D R and Seung H S 1989 *Phys. Rev. B* **39** 9153
- [52] Cule D and Hwa T 1996 *Phys. Rev. Lett.* **77** 278
- [53] Hwa T and Lässig M 1996 *Phys. Rev. Lett.* **76** 2591
- [54] Drasdo D, Hwa T and Lässig M 1998 *Preprint physics/9802023*
- [55] Hwa T and Lässig M 1998 *Proc. 2nd Annual Conf. on Computational Molecular Biology (RECOMB 98)*
(New York: ACM Press)
- [56] Drasdo D, Hwa T and Lässig M 1998 *Proc. 6th Int. Conf. on Intelligent Systems for Molecular Biology*
(ISMB 98) (Menlo Park, CA: AAAI Press)
- [57] Olsen R, Hwa T and Lässig M 1998 *Proc. Pacific Symp. on Biocomputing '99 (PSB 99)* at press
- [58] Lipowsky R 1991 *Europhys. Lett.* **15** 703
- [59] Duplantier B 1989 *Phys. Rev. Lett.* **62** 2337
- [60] Rajasekaran J J and Bhattacharjee S M 1991 *J. Phys. A: Math. Gen.* **24** L371
- [61] de Gennes P G 1968 *J. Chem. Phys.* **48** 2257

- Pokrovski V L and Talapov A L 1979 *Phys. Rev. Lett.* **42** 65
- [62] Redfield A C and Zangwill A 1992 *Phys. Rev. B* **46** 4289
- [63] Song S and Mochrie S G J 1994 *Phys. Rev. Lett.* **73** 995
- Song S and Mochrie S G J 1995 *Phys. Rev. B* **51** 10068
- [64] Lässig M 1996 *Phys. Rev. Lett.* **77** 526
- [65] van Dijken S, Zandvliet H J W and Poelsema B 1997 *Phys. Rev. B* **55** 7864
- van Dijken S, Zandvliet H J W and Poelsema B 1997 *Phys. Rev. B* **56** 1638
- Sudoh K, Yoshinobu T, Iwasaki H and Williams E 1998 *Phys. Rev. Lett.* **80** 5152
- [66] McKane A J and Moore M A 1988 *Phys. Rev. Lett.* **60** 527
- [67] Zhang Y-C 1989 *J. Stat. Phys.* **57** 1123
- [68] Feigel'man M V, Geshkenbein V B, Larkin A I and Vinokur V M 1989 *Phys. Rev. Lett.* **63** 2303
- [69] Nelson D and Le Doussal P 1990 *Phys. Rev. B* **42** 10113
- [70] Hwa T 1992 *Phys. Rev. Lett.* **69** 1552
- [71] Civalè L *et al* 1991 *Phys. Rev. Lett.* **67** 648
- [72] Budhani R C, Suenaga M and Lion S H 1992 *Phys. Rev. Lett.* **69** 3816
- [73] Tang L-H and Lyuksyutov I F 1993 *Phys. Rev. Lett.* **71** 2745
- [74] Balents L and Kardar M 1993 *Europhys. Lett.* **23** 503
- Balents L and Kardar M 1994 *Phys. Rev. B* **49** 13030
- [75] Kolomeisky E B and Straley J P 1995 *Phys. Rev. B* **51** 8030
- [76] Hwa T and Nattermann T 1994 *Phys. Rev. B* **51** 455
- [77] Mézard M 1990 *J. Physique* **51** 1831
- [78] Nattermann T, Feigel'man M and Lyuksyutov I 1991 *Z. Phys. B* **84** 353
- [79] Tang L-H 1994 *J. Stat. Phys.* **77** 581
- [80] Mukherji S 1994 *Phys. Rev. E* **50** R2407
- [81] Hwa T and Fisher D 1994 *Phys. Rev. B* **49** 3136
- [82] Lässig M, unpublished
- [83] Hwa T and Lässig M, unpublished
- [84] Krug J and Tang L-H 1994 *Phys. Rev. E* **50** 104
- [85] Willbrand K 1996 *Diploma Thesis* Technical University of Aachen
- [86] Mézard M and Parisi G 1991 *J. Physique I* **1** 809
- [87] Castellano C, Marsili M and Pietronero L 1998 *Phys. Rev. Lett.* **80** 3527
- [88] Wolf D E and Tang L-H 1990 *Phys. Rev. Lett.* **65** 1591
- [89] Martin P C, Siggia E D and Rose H A 1973 *Phys. Rev. A* **8** 423
- Bausch R, Janssen H K and Wagner H 1976 *Z. Phys. B* **24** 113
- [90] Sun T and Plischke M 1994 *Phys. Rev. E* **49** 5046
- [91] Wiese K J 1997 *Phys. Rev. E* **56** 5013
- [92] Wiese K J 1998 *J. Stat. Phys.* at press
- [93] Doty C A and Kosterlitz M 1992 *Phys. Rev. Lett.* **69** 1979
- [94] Lässig M 1990 *Nucl. Phys. B* **334** 652
- [95] Lässig M 1998 to be published
- [96] Chekhlov A and Yakhot V 1995 *Phys. Rev. E* **51** R2739
- [97] Kolmogorov A 1941 *Dokl. Acad. Nauk SSR* **32** 16 (Engl. Transl. 1991 *Proc. R. Soc. A* **434** 15)
- [98] Eyink G L 1993 *Phys. Lett.* **172A** 355
- [99] Polyakov A M 1995 *Phys. Rev. E* **52** 6183
- [100] Pelletier J D 1997 *Phys. Rev. Lett.* **78** 2672
- [101] Krug J 1994 *Phys. Rev. Lett.* **72** 2907
- [102] Lässig M 1998 *Preprint cond-mat/98*